J/ψ production in an equilibrating partonic system

Xiao-Ming Xu

Institute for Nuclear Theory, University of Washington, Box 351550,
Seattle, WA 98195
and
Nuclear Physics Division, Shanghai Institute of Nuclear Research
Chinese Academy of Sciences, P.O.Box 800204, Shanghai 201800, China

Abstract

Any color singlet or octet $c\bar{c}$ pair is created at short distances and then expands to a full size of J/ψ. Such a dynamical evolution process is included here in calculations for the J/ψ number distribution as a function of transverse momentum and rapidity in central Au-Au collisions at both RHIC and LHC energies. The $c\bar{c}$ pairs are produced in the initial collision and in the partonic system during the prethermal and thermal stages through the partonic channels $ab \to c\bar{c}[^{2S+1}L_J]$ and $ab \to c\bar{c}[^{2S+1}L_J]$x, and then they dissociate in the latter two stages. Dissociation of $c\bar{c}$ in the medium occurs via two reactions: (a) color singlet $c\bar{c}$ plus a gluon turns to color octet $c\bar{c}$, (b) color octet $c\bar{c}$ plus a gluon persists as color octet. There are modest yields of $c\bar{c}$ in the prethermal stage at RHIC energy and through the reactions $ab \to c\bar{c}[^{2S+1}L_J]$ at LHC energy for partons with large average momentum in the prethermal stage at both collider energies and in the thermal stage at LHC energy. Production from the partonic system competes with the suppression of the initial yield in the deconfined medium. Consequently, a bulge within $-1.5 < y < 1.5$ has been found for the J/ψ number distribution and the ratio of J/ψ number distributions for Au-Au collisions to nucleon-nucleon collisions. This bulge is caused by the partonic system and is thus an indicator of a deconfined partonic medium. Based on this result we suggest the rapidity region worth measuring in future experiments at RHIC and LHC to be $-3 < y < 3$.

PACS codes: 24.85.+p, 12.38.Mh, 25.75.Dw, 25.75.Gz
Keywords: Ultrarelativistic nucleus-nucleus collisions, Equilibrating partonic system, J/ψ number distribution, Survival probability

1. Introduction

A hot deconfined medium favors the dissociation of J/ψ since enough hard gluons can overcome the large energy gap between the J/ψ and a continuum state of $c\bar{c}$ [1]. Models based on perturbative QCD have shown that a dense partonic system can be produced in central Au-Au collisions at RHIC and LHC energies [2-6] and then evolve toward thermal equilibrium and likely chemical equilibrium [7-11]. Such parton plasmas will be searched for soon in experiments at Brookhaven National Laboratory Relativistic Heavy Ion Collider (RHIC). The J/ψ suppression has been taken as a thermometer to identify the evolution history of a parton plasma by showing transverse momentum dependence of the survival probability in the central rapidity region [12].

Charmonium melting inside a hot medium, which leads to J/ψ suppression, was proposed by Matsui and Satz to probe the existence of the quark-gluon plasma [13]. Before the complete formation of charmonium is achieved, a pre-resonant $c\bar{c}$ is expanding from a collision point. Dominance of the color octet plus a collinear gluon configuration in the pre-resonance state [14] may account for the same suppression of ψ' and J/ψ production in proton-nucleus collisions [15]. The growth of the color octet configuration and its interaction with nucleons along its trajectory in a nucleus are essential ingredients in explaining measured J/ψ production cross sections. In addition, the importance of color octet configurations has been verified in $p\bar{p}$ collisions at center-of-mass energy $\sqrt{s} = 1.8$ TeV with the CDF detector at Fermilab [16]. Theoretically, the color-octet production at short distances and its evolution into physical resonances has been well formulated in nonrelativistic QCD [17]. At the collision energies of RHIC and LHC we can reasonably expect considerable contributions from the color octet mechanism.

The evolution of ultrarelativistic nucleus-nucleus collisions, e.g. central Au-Au collisions at both RHIC and LHC energies, has been divided into three stages in Refs. [9,18,19]: (a) an initial collision where a parton gas is produced; (b) a prethermal stage where elastic scatterings among partons lead to local momentum isotropy [20]; (c) a thermal stage where parton numbers increase until freeze-out. The term 'partonic system' refers to the assembly of partons in the prethermal and thermal stages. The parton plasma only denotes the assembly of partons in the thermal stage. The $c\bar{c}$ pairs are produced in the initial collision, prethermal and thermal stages but disintegrate in the latter two stages. In order to understand and make predictions for J/ψ yields of RHIC and LHC experiments, the following physical processes are taken into account. (a) In the initial collision, $c\bar{c}$ pairs are produced in hard and semihard scatterings between partons from incoming nuclei by $2 \to 2$ processes which start at order α_s^3 through the partonic channels $ab \to c\bar{c}[^{2S+1}L_J]$x. In the prethermal and thermal stages, $c\bar{c}$ pairs can also be produced in $2 \to 1$ collisions which start at order α_s^2 via the partonic channels $ab \to c\bar{c}[^{2S+1}L_J]$ since partons in the deconfined medium have large transverse momenta. (b) The $c\bar{c}$ produced at short distance is in a color singlet $(c\bar{c})_1$ or color octet $(c\bar{c})_8$ configuration which has a certain probability to evolve nonperturbatively into a color singlet state. This J/ψ production process is formulated in nonrelativistic QCD. (c) Since the color octet to singlet transition of $(c\bar{c})_8$ takes time, gluons in the partonic medium couple to the color octet state and destroy this transition process. Normally, dissociation cross sections for $g + c\bar{c} \to (c\bar{c})_8$ depend on the pair size. Expansion of the $c\bar{c}$ from a collision point to a full J/ψ size has to be taken into account.

A physical resonance formed by a $c\bar{c}$ pair may be one of J/ψ, χ_{cJ}, ψ' and others. Since the radiative transition from a higher charmonium state to the J/ψ takes a much longer time, the transition of such a state with nonzero p_T takes place outside the partonic system. Since the Fermilab Tevatron experiments have been able to separate direct J/ψ's from those produced in radiative χ_{cJ} decays [16], in this work we assume that the direct J/ψ production can also be extracted in heavy ion measurements. If χ_{cJ} and ψ' are considered, suppression factors for χ_{cJ} and ψ' in a deconfined medium are included in prompt J/ψ production. The identification of J/ψ suppression in the medium becomes impossible for any prompt J/ψ production data. Therefore, no contributions from higher charmonium states are taken into account in this work.

The purpose of this work is to study the dependence of the J/ψ survival probability and number distributions produced in central Au-Au collisions at RHIC and LHC energies on the transverse momentum and also rapidity which will be measured in RHIC experiments [21]. The J/ψ number distributions corresponding to production of $c\bar{c}$ in the initial collision are given in Section 2. Since nuclear shadowing has been shown to influence J/ψ production in proton-nucleus collisions [22], the nuclear modification of parton distributions is considered. The J/ψ number distributions due to $c\bar{c}$ production in the prethermal and thermal stages are given in Sections 3 and 4. Section 5 contains dissociation cross sections for gluon-$(c\bar{c})_1$ and gluon-$(c\bar{c})_8$. Numerical results for nucleon-$c\bar{c}$ cross sections, J/ψ number distributions and four ratios including survival probability are presented in Section 6. Conclusions are summarized in the final section.

2. Initial production of $c\bar{c}$

Intrinsic transverse momenta of partons inside a nucleon result in the production of J/ψ with typical momenta comparable to the QCD scale via $2 \to 1$ partonic scattering processes [23]. Since we want to study J/ψ productions with $p_T > 2$ GeV, contributions from $2 \to 1$ partonic reactions are not considered in the initial nucleon-nucleon collision. The effect of intrinsic transverse momentum smearing is rather modest for large transverse momentum J/ψ data from the Tevatron [24]. Upon omission of the intrinsic transverse momentum, differential cross section for J/ψ production in nucleon-nucleon collision resulting only from $2 \to 2$ partonic processes is given as

$$\begin{aligned}\frac{d^3\sigma}{dydy_{\rm x}dp_\perp} &= 2p_\perp \sum_{ab{\rm x}} x_a x_b f_{a/N}(x_a) f_{b/N}(x_b) \\ &\quad [\sum_{(1)} \frac{d\sigma}{dt}(ab \to c\bar{c}[^{2S+1}L_J^{(1)}]{\rm x} \to J/\psi) \\ &\quad + \sum_{(8)} \frac{d\sigma}{dt}(ab \to c\bar{c}[^{2S+1}L_J^{(8)}]{\rm x} \to J/\psi)] \end{aligned} \quad (1)$$

where the summation $\sum_{ab{\rm x}}$ is over partons labeled by $a, b, {\rm x}$, $\sum_{(1)}$ for all possible color-singlet states and $\sum_{(8)}$ for all possible color-octet states. Here $\frac{d\sigma}{dt}$ denotes the partonic differential cross section for producing a $c\bar{c}[^{2S+1}L_J]$ and evolving to a J/ψ with spectroscopic notation for quantum numbers and superscripts for singlet and octet [23, 25], and $f_{a/N}$ is the parton distribution function of the species a in a free nucleon. The longitudinal momentum fractions carried by initial partons, x_a and x_b, are related to rapidities of $c\bar{c}$

and x, y and $y_{\rm x}$, by

$$x_a = \frac{1}{\sqrt{s}}(m_\perp e^{y} + p_\perp e^{y_{\rm x}}), \qquad\qquad x_b = \frac{1}{\sqrt{s}}(m_\perp e^{-y} + p_\perp e^{-y_{\rm x}})$$

where $\sqrt{s}$, $p_\perp$ and $m_\perp$ are the center-of-mass energy of nucleon-nucleon collision, transverse momentum and transverse mass of the J/ψ. The conditions $x_a < 1$ and $x_b < 1$ restrict $y_{\rm x}$ to a region of

$$-\ln\frac{\sqrt{s}-m_\perp e^{-y}}{p_\perp} < y_{\rm x} < \ln\frac{\sqrt{s}-m_\perp e^{y}}{p_\perp}$$

These $2\to 2$ processes at order α_s^3, $gg \to c\bar{c}[^{2S+1}L_J]g$, $q\bar{q} \to c\bar{c}[^{2S+1}L_J]g$, $gq \to c\bar{c}[^{2S+1}L_J]q$ and $g\bar{q} \to c\bar{c}[^{2S+1}L_J]\bar{q}$, start in initial nucleus-nucleus collisions and proceed with the expansion of the heavy pair. While a $c\bar{c}$ propagates inside a prethermal or thermal partonic system, gluons hit and excite it to continuum states. Let $\sigma_{gc\bar{c}[^1S_1^{(1)}]}$ be the cross section for $g+(c\bar{c})[1^3S_1^{(1)}] \to (c\bar{c})_8$, $\sigma_{gc\bar{c}[S^{(8)}]}$ for $g+(c\bar{c})[S^{(8)}] \to (c\bar{c})_8$ and $\sigma_{gc\bar{c}[P^{(8)}]}$ for $g+(c\bar{c})[P^{(8)}] \to (c\bar{c})_8$ respectively. The cross sections are calculated in Section 5. The probability for dissociation of a small-size $c\bar{c}$ into a free state relies on the relative velocity between the gluon and $c\bar{c}$, v_{rel}, and gluon number densities in the prethermal and thermal stages, $n_g(x)$ and $n_g(\tau)$, respectively. Here the variables x and τ are individually space-time coordinates and proper time. In the prethermal stage, parton distributions depend on the correlation between momentum and space-time coordinates [18, 19]. The dependence of the gluon number density $n_g(x)$ on x characterizes the partonic system in nonequilibrium. In the thermal stage, thermal parton distributions can be approximated by Jüttner distributions where the temperature and parton fugacities depend only on the proper time [9, 18, 20]. As a consequence, the gluon number density is only a function of τ. Including $c\bar{c}$ suppression in the partonic system, the finally-formed number distribution of J/ψ resulting from $c\bar{c}$ pairs produced in the initial central A+B collision is given by

$$\begin{aligned}
\frac{dN_{ini}^{2\to 2}}{dyd^2p_\perp} &= 2\int_{-\ln\frac{\sqrt{s}-m_\perp e^{-y}}{p_\perp}}^{\ln\frac{\sqrt{s}-m_\perp e^{y}}{p_\perp}} dy_{\rm x}\int_0^{R_A} drr \\
&\sum x_a f_{a/A}(x_a, m_\perp^2, \vec{r}) x_b f_{b/B}(x_b, m_\perp^2, -\vec{r}) \\
&\{\frac{d\sigma}{dt}(ab \to c\bar{c}[^3S_1^{(1)}]{\rm x} \to J/\psi) \\
&\exp[-\int_{\tau_0}^{\tau_{iso}} d\tau' n_g(x') < v_{rel}\sigma_{gc\bar{c}[^1S_1^{(1)}]}(k\cdot u) >_{pre} \theta(d - V_T\Delta t) \\
&-\int_{\tau_{iso}}^{\tau_f} d\tau' n_g(\tau') < v_{rel}\sigma_{gc\bar{c}[^1S_1^{(1)}]}(k\cdot u) >_{the} \theta(d - V_T\Delta t)] \\
&+\frac{d\sigma}{dt}(ab \to c\bar{c}[^3S_1^{(8)}]{\rm x} \to J/\psi) \\
&\exp[-\int_{\tau_0}^{\tau_{iso}} d\tau' n_g(x') < v_{rel}\sigma_{gc\bar{c}[S^{(8)}]}(k\cdot u) >_{pre} \theta(d - V_T\Delta t) \\
&-\int_{\tau_{iso}}^{\tau_f} d\tau' n_g(\tau') < v_{rel}\sigma_{gc\bar{c}[S^{(8)}]}(k\cdot u) >_{the} \theta(d - V_T\Delta t)] \\
&+\frac{d\sigma}{dt}(ab \to c\bar{c}[^1S_0^{(8)}]{\rm x} \to J/\psi)
\end{aligned}$$

$$
\begin{aligned}
&\exp[-\int_{\tau_0}^{\tau_{iso}} d\tau' n_g(x') < v_{rel}\sigma_{gc\bar{c}[S^{(8)}]}(k\cdot u) >_{pre} \theta(d - V_T\Delta t) \\
&-\int_{\tau_{iso}}^{\tau_f} d\tau' n_g(\tau') < v_{rel}\sigma_{gc\bar{c}[S^{(8)}]}(k\cdot u) >_{the} \theta(d - V_T\Delta t)] \\
&+\frac{d\sigma}{dt}(ab \to c\bar{c}[^3P_J^{(8)}]\mathrm{x} \to J/\psi) \\
&\exp[-\int_{\tau_0}^{\tau_{iso}} d\tau' n_g(x') < v_{rel}\sigma_{gc\bar{c}[P^{(8)}]}(k\cdot u) >_{pre} \theta(d - V_T\Delta t) \\
&-\int_{\tau_{iso}}^{\tau_f} d\tau' n_g(\tau') < v_{rel}\sigma_{gc\bar{c}[P^{(8)}]}(k\cdot u) >_{the} \theta(d - V_T\Delta t)]\}
\end{aligned}
\tag{2}
$$

where $f_{a/A}$ is the parton distribution function of a nucleus,

$$
f_{a/A}(x, Q^2, \vec{r}) = T_A(\vec{r}) S_{a/A}(x, \vec{r}) f_{a/N}(x, Q^2) \tag{3}
$$

with the thickness function T_A and nuclear parton shadowing factor $S_{a/A}$. Here, R_A is the nuclear radius. The symbols $< \cdots >_{pre}$ and $< \cdots >_{the}$ denote averages over gluon distributions in the prethermal and thermal stages, respectively. Along the track of nucleus-nucleus collisions, a deconfined partonic gas is produced from scatterings among primary partons at τ_0, then reaches thermalization at τ_{iso} and finally freezes out at τ_f. Here, d is the shortest distance which a $c\bar{c}$ travels from a production point $\vec{r}$ to the surface of the partonic medium with transverse velocity V_T [12]. Suppose a $c\bar{c}$ is produced at a proper time τ and a spatial rapidity η. The time Δt for the partonic system to evolve to another proper time τ' is

$$
\Delta t = \frac{(V_\parallel \sinh\eta - \cosh\eta)\tau + \sqrt{(\sinh\eta - V_\parallel \cosh\eta)^2\tau^2 + (1 - V_\parallel^2)\tau'^2}}{1 - V_\parallel^2} \tag{4}
$$

where $V_\parallel$ is the longitudinal component of the $c\bar{c}$ velocity. The disappearance of medium interactions on the $c\bar{c}$ is ensured by the step function θ while this pair escapes from the partonic medium.

3. Production of $c\bar{c}$ in the prethermal stage

To order α_s^2, a $c\bar{c}$ in a color singlet state is produced only through gluon fusion $gg \to c\bar{c}[^{2S+1}L_J^{(1)}]$. For the $c\bar{c}[^3S_1^{(1)}]$, this fusion does not occur. In contrast, color octet states result from both channels $gg \to c\bar{c}[^{2S+1}L_J^{(8)}]$ and $q\bar{q} \to c\bar{c}[^{2S+1}L_J^{(8)}]$. Nevertheless, the number densities of quarks and antiquarks are so small that they are neglected in estimating the production of $c\bar{c}$ in the prethermal stage where gluons dominate the partonic system. Four momenta of the two initial partons and final $c\bar{c}$ are denoted by $k_1 = (\omega_1, \vec{k}_1)$, $k_2 = (\omega_2, \vec{k}_2)$ and $p = (E, \vec{p}) = (m_\perp \cosh y, \vec{p}_\perp, m_\perp \sinh y)$. The differential production rate for $gg \to c\bar{c}[^{2S+1}L_J^{(8)}] \to J/\psi$ in the prethermal stage is

$$
\begin{aligned}
E\frac{d^3A_{pre}^{2\to1}}{d^3p} &= \frac{1}{8(2\pi)^5}\int \frac{d^3k_1}{\omega_1}\frac{d^3k_2}{\omega_2}\delta^{(4)}(k_1 + k_2 - p)\frac{1}{2}g_G^2 f_g(k_1, x) f_g(k_2, x) \\
&\sum_{(8)} \mid \mathcal{M}(gg \to c\bar{c}[^{2S+1}L_J^{(8)}] \to J/\psi) \mid^2
\end{aligned}
\tag{5}
$$

where g_G is the degeneracy factor for gluons and the $f_g(k,x)$ is the correlated phase-space distribution function given in Ref. [18]. The squared amplitudes $\mid \mathcal{M} \mid^2$ for $c\bar{c}$ in color singlet and color octet are calculated individually in Refs. [23, 25]. To order α_s^2, the allowed color octet states are ${}^1S_0^{(8)}$ and ${}^3P_{0,2}^{(8)}$ through the gluon fusion channel. Taking into account the suppression of $c\bar{c}$ in the prethermal and thermal stages, the finally-formed number distribution of J/ψ resulting from $c\bar{c}$ pairs produced through $2 \to 1$ processes in the prethermal stage is given by

$$\begin{aligned}
\frac{dN_{pre}^{2\to 1}}{dyd^2p_\perp} &= \frac{\pi R_A^2}{16(2\pi)^5}\int_{\tau_0}^{\tau_{iso}} \tau d\tau d\eta d\phi_{k_1} dy_{k_1} \frac{k_{\perp 1}^2}{m_c^2}\frac{1}{2} g_G^2 f_g(k_1,x) f_g(k_2,x) \\
&\{\mid \mathcal{M}(gg \to c\bar{c}[{}^1S_0^{(8)}] \to J/\psi) \mid^2 \\
&\exp[-\int_\tau^{\tau_{iso}} d\tau' n_g(x') < v_{rel}\sigma_{gc\bar{c}[S^{(8)}]}(k\cdot u) >_{pre} \theta(d - V_T\Delta t) \\
&-\int_{\tau_{iso}}^{\tau_f} d\tau' n_g(\tau') < v_{rel}\sigma_{gc\bar{c}[S^{(8)}]}(k\cdot u) >_{the} \theta(d - V_T\Delta t)] \\
&+ \mid \mathcal{M}(gg \to c\bar{c}[{}^3P_J^{(8)}] \to J/\psi) \mid^2 \\
&\exp[-\int_\tau^{\tau_{iso}} d\tau' n_g(x') < v_{rel}\sigma_{gc\bar{c}[P^{(8)}]}(k\cdot u) >_{pre} \theta(d - V_T\Delta t) \\
&-\int_{\tau_{iso}}^{\tau_f} d\tau' n_g(\tau') < v_{rel}\sigma_{gc\bar{c}[P^{(8)}]}(k\cdot u) >_{the} \theta(d - V_T\Delta t)]\}
\end{aligned} \tag{6}$$

where ϕ_{k_i} is the angle between $\vec{k}_{\perp i}$ and $\vec{p}_\perp$ for $i = 1, 2$ and m_c is the charm quark mass. The kinematic variables $k_{\perp 1}$, $k_{\perp 2}$, ϕ_{k_2} and y_{k_2} are expressed in terms of

$$k_{\perp 1} = \frac{2m_c^2}{m_\perp \cosh(y - y_{k_1}) - p_\perp \cos\phi_{k_1}}$$

$$k_{\perp 2} = \sqrt{p_\perp^2 + k_{\perp 1}^2 - 2p_\perp k_{\perp 1}\cos\phi_{k_1}}$$

$$\sin\phi_{k_2} = -\frac{k_{\perp 1}}{k_{\perp 2}}\sin\phi_{k_1}$$

$$\sinh y_{k_2} = \frac{1}{k_{\perp 2}}(m_\perp \sinh y - k_{\perp 1}\sinh y_{k_1})$$

To order α_s^3, the differential production rate gets contributions from the processes $gg \to c\bar{c}[{}^{2S+1}L_J^{(1,8)}]g$ in the prethermal stage,

$$\begin{aligned}
E\frac{d^3A_{pre}^{2\to 2}}{d^3p} &= \frac{1}{16(2\pi)^8}\int \frac{d^3k_1}{\omega_1}\frac{d^3k_2}{\omega_2}\frac{d^3p_{\rm x}}{E_{\rm x}}\delta^{(4)}(k_1 + k_2 - p - p_{\rm x}) \\
&\frac{1}{2}g_G^2 f_g(k_1,x) f_g(k_2,x)\{\sum_{(1)} \mid \mathcal{M}(gg \to c\bar{c}[{}^{2S+1}L_J^{(1)}]{\rm x} \to J/\psi) \mid^2 \\
&+ \sum_{(8)} \mid \mathcal{M}(gg \to c\bar{c}[{}^{2S+1}L_J^{(8)}]{\rm x} \to J/\psi) \mid^2\}
\end{aligned} \tag{7}$$

where $p_{\rm x} = (E_{\rm x}, \vec{p}_{\rm x}) = (p_{\perp{\rm x}}\cosh y_{\rm x}, p_{\perp{\rm x}}\cos\phi_{\rm x}, p_{\perp{\rm x}}\sin\phi_{\rm x}, p_{\perp{\rm x}}\sinh y_{\rm x})$ is the four momentum of the massless parton x. Taking into account the suppression of $c\bar{c}$ in the prethermal

and thermal stages, the finally-formed number distribution of J/ψ resulting from $c\bar{c}$ pairs produced through $2 \to 2$ processes in the prethermal stage is given by

$$\begin{aligned}
\frac{dN_{pre}^{2\to 2}}{dyd^2p_\perp} &= \frac{\pi R_A^2}{16(2\pi)^8}\int_{\tau_0}^{\tau_{iso}} \tau d\tau d\eta p_{\perp \mathrm{x}} dp_{\perp \mathrm{x}} d\phi_{\mathrm{x}} dy_{\mathrm{x}} d\phi_{k_1} dy_{k_1} \\
&\frac{2k_{\perp 1}^2}{\hat{s}}\frac{1}{2} g_G^2 f_g(k_1,x) f_g(k_2,x) \\
&\{\mid \mathcal{M}(gg \to c\bar{c}[^3S_1^{(1)}]\mathrm{x} \to J/\psi) \mid^2 \\
&\exp[-\int_\tau^{\tau_{iso}} d\tau' n_g(x') < v_{rel}\sigma_{gc\bar{c}[1^3S_1^{(1)}]}(k\cdot u) >_{pre} \theta(d - V_T\Delta t) \\
&- \int_{\tau_{iso}}^{\tau_f} d\tau' n_g(\tau') < v_{rel}\sigma_{gc\bar{c}[1^3S_1^{(1)}]}(k\cdot u) >_{the} \theta(d - V_T\Delta t)] \\
&+ \mid \mathcal{M}(gg \to c\bar{c}[^3S_1^{(8)}]\mathrm{x} \to J/\psi) \mid^2 \\
&\exp[-\int_\tau^{\tau_{iso}} d\tau' n_g(x') < v_{rel}\sigma_{gc\bar{c}[S^{(8)}]}(k\cdot u) >_{pre} \theta(d - V_T\Delta t) \\
&- \int_{\tau_{iso}}^{\tau_f} d\tau' n_g(\tau') < v_{rel}\sigma_{gc\bar{c}[S^{(8)}]}(k\cdot u) >_{the} \theta(d - V_T\Delta t)] \\
&+ \mid \mathcal{M}(gg \to c\bar{c}[^1S_0^{(8)}]\mathrm{x} \to J/\psi) \mid^2 \\
&\exp[-\int_\tau^{\tau_{iso}} d\tau' n_g(x') < v_{rel}\sigma_{gc\bar{c}[S^{(8)}]}(k\cdot u) >_{pre} \theta(d - V_T\Delta t) \\
&- \int_{\tau_{iso}}^{\tau_f} d\tau' n_g(\tau') < v_{rel}\sigma_{gc\bar{c}[S^{(8)}]}(k\cdot u) >_{the} \theta(d - V_T\Delta t)] \\
&+ \mid \mathcal{M}(gg \to c\bar{c}[^3P_J^{(8)}]\mathrm{x} \to J/\psi) \mid^2 \\
&\exp[-\int_\tau^{\tau_{iso}} d\tau' n_g(x') < v_{rel}\sigma_{gc\bar{c}[P^{(8)}]}(k\cdot u) >_{pre} \theta(d - V_T\Delta t) \\
&- \int_{\tau_{iso}}^{\tau_f} d\tau' n_g(\tau') < v_{rel}\sigma_{gc\bar{c}[P^{(8)}]}(k\cdot u) >_{the} \theta(d - V_T\Delta t)]\}
\end{aligned} \tag{8}$$

where $\hat{s} = (k_1 + k_2)^2$ and some kinematic variables are given by

$$k_{\perp 1} = \{4m_c^2 + 2m_\perp p_{\perp \mathrm{x}} \cosh(y - y_{\mathrm{x}}) - 2p_\perp p_{\perp \mathrm{x}} \cos\phi_{\mathrm{x}}\}/$$

$$\{2[m_\perp \cosh(y - y_{k_1}) + p_{\perp \mathrm{x}} \cosh(y_{\mathrm{x}} - y_{k_1}) - p_\perp \cos\phi_{k_1} - p_{\perp \mathrm{x}} \cos(\phi_{\mathrm{x}} - \phi_{k_1})]\}$$

$$\begin{aligned}
k_{\perp 2}^2 &= m_\perp^2 + p_{\perp \mathrm{x}}^2 + 2m_\perp p_{\perp \mathrm{x}} \cosh(y - y_{\mathrm{x}}) + k_{\perp 1}^2 \\
&\quad -2k_{\perp 1}[m_\perp \cosh(y - y_{k_1}) + p_{\perp \mathrm{x}} \cosh(y_{\mathrm{x}} - y_{k_1})]
\end{aligned}$$

$$\sinh y_{k_2} = \frac{1}{k_{\perp \mathrm{x}}}[m_\perp \sinh y + p_{\perp \mathrm{x}} \sinh y_{\mathrm{x}} - k_{\perp 1} \sinh y_{k_1}]$$

The J/ψ number distribution resulting from $c\bar{c}$ pairs produced in the prethermal stage becomes

$$\frac{dN_{pre}}{dyd^2p_\perp} = \frac{dN_{pre}^{2\to 1}}{dyd^2p_\perp} + \frac{dN_{pre}^{2\to 2}}{dyd^2p_\perp} \tag{9}$$

4. Production of $c\bar{c}$ in the thermal stage

In the thermal stage, parton distributions are approximated by thermal phase-space distributions $f_i(k;T,\lambda_i)$ in which the temperature T and nonequilibrium fugacities λ_i are functions of the proper time τ [9, 18]. While the partonic system evolves, quark and antiquark number densities increase. To order α_s^2, both $gg \to c\bar{c}[^{2S+1}L_J^{(8)}] \to J/\psi$ and $q\bar{q} \to c\bar{c}[^{2S+1}L_J^{(8)}] \to J/\psi$ contribute to the J/ψ number distribution in the thermal stage

$$\begin{aligned}
\frac{dN_{the}^{2\to 1}}{dyd^2p_\perp} &= \frac{\pi R_A^2}{16(2\pi)^5}\int_{\tau_{iso}}^{\tau_f}\tau d\tau d\eta d\phi_{k_1}dy_{k_1}\frac{k_{\perp 1}^2}{m_c^2} \\
&\{\frac{1}{2}g_G^2 f_g(k_1;T,\lambda_g)f_g(k_2;T,\lambda_g) \mid \mathcal{M}(gg\to c\bar{c}[^1S_0^{(8)}]\to J/\psi)\mid^2 \\
&\exp[-\int_\tau^{\tau_f} d\tau' n_g(\tau') < v_{rel}\sigma_{gc\bar{c}[S^{(8)}]}(k\cdot u) >_{the} \theta(d-V_T\Delta t)] \\
&+\frac{1}{2}g_G^2 f_g(k_1;T,\lambda_g)f_g(k_2;T,\lambda_g) \mid \mathcal{M}(gg\to c\bar{c}[^3P_J^{(8)}]\to J/\psi)\mid^2 \\
&\exp[-\int_\tau^{\tau_f} d\tau' n_g(\tau') < v_{rel}\sigma_{gc\bar{c}[P^{(8)}]}(k\cdot u) >_{the} \theta(d-V_T\Delta t)] \\
&+g_q g_{\bar{q}} f_q(k_1;T,\lambda_q)f_{\bar{q}}(k_2;T,\lambda_{\bar{q}}) \mid \mathcal{M}(q\bar{q}\to c\bar{c}[^3S_1^{(8)}]\to J/\psi)\mid^2 \\
&\exp[-\int_\tau^{\tau_f} d\tau' n_g(\tau') < v_{rel}\sigma_{gc\bar{c}[S^{(8)}]}(k\cdot u) >_{the} \theta(d-V_T\Delta t)]\}
\end{aligned} \tag{10}$$

where g_q and $g_{\bar{q}}$ are the degeneracy factors for quarks and antiquarks, respectively. In the channel of quark-antiquark annihilation, only the squared amplitude for $^3S_1^{(8)}$ does not vanish.

All lowest-order $2 \to 2$ reactions $gg \to c\bar{c}[^{2S+1}L_J]g$, $q\bar{q} \to c\bar{c}[^{2S+1}L_J]g$, $gq \to c\bar{c}[^{2S+1}L_J]q$ and $g\bar{q} \to c\bar{c}[^{2S+1}L_J]\bar{q}$ contribute to the J/ψ number distribution in the thermal stage

$$\begin{aligned}
\frac{dN_{the}^{2\to 2}}{dyd^2p_\perp} &= \frac{\pi R_A^2}{16(2\pi)^8}\int_{\tau_{iso}}^{\tau_f}\tau d\tau d\eta p_{\perp \mathrm{x}} dp_{\perp \mathrm{x}} d\phi_{\mathrm{x}} dy_{\mathrm{x}} d\phi_{k_1} dy_{k_1}\frac{2k_{\perp 1}^2}{\hat{s}} \\
&\sum_{ab}\frac{1}{2}f_a(k_1;T,\lambda_a)f_b(k_2;T,\lambda_b)g_a g_b \\
&\{\sum_{(1)} \mid \mathcal{M}(ab\to c\bar{c}[^{2S+1}L_J^{(1)}]\mathrm{x}\to J/\psi)\mid^2 \\
&\exp[-\int_\tau^{\tau_f} d\tau' n_g(\tau') < v_{rel}\sigma_{gc\bar{c}[1^{2S+1}L_J^{(1)}]}(k\cdot u) >_{the} \theta(d-V_T\Delta t)] \\
&+\sum_{(8)} \mid \mathcal{M}(ab\to c\bar{c}[^{2S+1}L_J^{(8)}]\mathrm{x}\to J/\psi)\mid^2 \\
&\exp[-\int_\tau^{\tau_f} d\tau' n_g(\tau') < v_{rel}\sigma_{gc\bar{c}[L^{(8)}]}(k\cdot u) >_{the} \theta(d-V_T\Delta t)]\}
\end{aligned} \tag{11}$$

The J/ψ number distribution resulting from $c\bar{c}$ pairs produced in the thermal stage becomes

$$\frac{dN_{the}}{dyd^2p_\perp} = \frac{dN_{the}^{2\to 1}}{dyd^2p_\perp} + \frac{dN_{the}^{2\to 2}}{dyd^2p_\perp} \tag{12}$$

5. Gluon-$c\bar{c}$ dissociation cross sections

A dissociation cross section of a full-size J/ψ induced by a gluon is given in Refs. [1, 26]. Since an initially-created $c\bar{c}$ has a radius of about $r_0 = \frac{1}{2m_c}$ and proceeds by expanding to a full-size object, the dissociation cross section of $c\bar{c}$ by a gluon has a size dependence. By this we mean the dissociation of $c\bar{c}$ into free states via this process $g + c\bar{c} \to (c\bar{c})_8$. Cross sections are calculated with chromoelectric dipole coupling between gluon and $c\bar{c}$ in the procedure for gluon-J/ψ dissociation in Ref. [26]. The wave function of an expanding $c\bar{c}$ is needed for this purpose, but it has not been investigated in the partonic medium even though some attempts have been made in studies of the color transparency phenomenon [27]. We proceed with the construction of wave functions in a simple one-gluon-exchange potential model.

In a parton plasma, the internal motion of J/ψ is obtained [12] from the attractive Coulomb potential, $V_1 = -{g_s}^2/3\pi r$. The quantum-mechanical interpretation of the $c\bar{c}$ radius is $\sqrt{< r^2 >}$, the square root of the radius-square expectation value of the relative-motion wave function. For the 1S color singlet, its wave function in momentum space normalized to the radius of $c\bar{c}[1^3S_1^{(1)}]$ is

$$[\vec{r}\psi_{1s}](\vec{k}) = 32\sqrt{\pi}a_0^{2.5}\frac{\vec{k}a_0}{(1+(ka_0)^2)^3} \tag{13}$$

where the variable $a_0 = \sqrt{< r^2 > /3}$ is the Bohr radius for a full-size J/ψ. The velocity-square expectation value of the J/ψ wave function is $< v^2 >= 0.428$. Then the radius of $c\bar{c}$ is assumed to expand according to $\sqrt{< r^2 >} = \sqrt{< v^2 >}t + r_0$. The gluon-$c\bar{c}[1^3S_1^{(1)}]$ dissociation cross section is

$$\sigma_{gc\bar{c}[1^3S_1^{(1)}]} = \frac{128{g_s}^2 m_c^{2.5} a_0^7 (Q^0-\epsilon_0)^{1.5} Q^0}{9[m_c a_0^2(Q^0-\epsilon_0)+1]^6} \tag{14}$$

where Q^0 is the gluon energy, ϵ_0 the binding energy of J/ψ and g_s the strong coupling constant.

While the $c\bar{c}$ is in a color octet state, it is not a bound state but rather a scattering state. Its relative-motion wave function is determined by the repulsive potential $V_8 = g_s^2/24\pi r$. The radial part of the S wave function is

$$S_R(r) + iS_I(r) = e^{iqr}F(1+i\eta, 2, -2iqr) \tag{15}$$

and the radial part of the P wave function is

$$P_R(r) + iP_I(r) = qre^{iqr}F(2+i\eta, 4, -2iqr) \tag{16}$$

with $q = m_c\sqrt{< v^2 >}$ and $\eta = g_s^2/24\pi\sqrt{< v^2 >}$. The function F is the confluent hypergeometric function. Wave functions in momentum space are obtained by performing a Fourier transform of the wave functions in space coordinates. Normalization constants of the momentum-space wave functions, C_S and C_P, are determined by fitting the $c\bar{c}$ radius. Dissociation cross sections of the S-wave and P-wave color-octet states by a gluon are

$$\begin{aligned}\sigma_{gc\bar{c}[S^{(8)}]} &= \frac{g_s^2(m_cQ^0)^{1.5}}{576\pi}C_S^2\int_0^b\int_0^b dr_1dr_2r_1^3r_2^3 \\ &\quad j_1(\sqrt{m_cQ^0}r_1)j_1(\sqrt{m_cQ^0}r_2)[S_R(r_1)S_R(r_2)+S_I(r_1)S_I(r_2)]\end{aligned} \tag{17}$$

$$\sigma_{gc\bar{c}[P^{(8)}]} = \frac{g_s^2(m_cQ^0)^{1.5}}{576\pi}C_P^2\int_0^b\int_0^b dr_1dr_2\frac{r_1^3r_2^3}{6\pi^2} [j_0(\sqrt{m_cQ^0}r_1)j_0(\sqrt{m_cQ^0}r_2)+2j_2(\sqrt{m_cQ^0}r_1)j_2(\sqrt{m_cQ^0}r_2)] [P_R(r_1)P_R(r_2)+P_I(r_1)P_I(r_2)] \quad (18)$$

where the j_0, j_1 and j_2 are spherical Bessel functions. The b is determined so that the square root of the r^2 expectation value of the relative wave function in Eq. (15) or (16) is the color-octet radius. Relations $b = 1.435\sqrt{< r^2 >}$ for S-wave and $b = 1.3\sqrt{< r^2 >}$ for P-wave approximately hold for color-octet size less than normal hadron size.

6. Numerical results and discussions

Results for five aspects are presented in the following subsections. The first aspect is the nucleon-$c\bar{c}$ dissociation cross sections shown in the next subsection. The second one in Subsection 6.2 is J/ψ number distributions versus transverse momentum at $y = 0$ and rapidity at $p_T = 4$ GeV with nuclear effect on parton distributions and $c\bar{c}$ dissociation in the partonic system. The third one in Subsection 6.3 is to define and calculate four ratios including survival probability with $y = 0$ or $p_T = 4$ GeV at both RHIC and LHC energies. The fourth one is given in Subsection 6.4 to show J/ψ number distributions without nuclear effect on parton distributions and $c\bar{c}$ dissociation in the partonic system. The fifth one concerns some uncertainties on the above results.

6.1. Nucleon-$c\bar{c}$ dissociation cross sections

In the parton model of the nucleon, the gluon is a dominant ingredient. Whereas the cross section for $c\bar{c}$ dissociated directly by a real gluon is of order α_s, the cross section for the quark-$c\bar{c}$ dissociation through a virtual gluon is of order α_s^2. With the gluon-$(c\bar{c})_1$ cross section given in the last section, the nucleon-$c\bar{c}[1^3S_1^{(1)}]$ cross section driven mainly by the gluon ingredient becomes

$$\sigma_{Nc\bar{c}[1^3S_1^{(1)}]} = \int_{x_{min}^{(1)}}^1 dx f_{g/N}(x,Q^2)\sigma_{gc\bar{c}[1^3S_1^{(1)}]} \quad (19)$$

where $x_{min}^{(1)} = \frac{\epsilon_0}{p_N}$ with p_N being the proton momentum in the rest frame of the J/ψ. The gluon distribution function $f_{g/N}$ is that Glück-Reya-Vogt (GRV) result at leading order in Ref. [28]. The cross section is drawn in Fig. 1 to show the energy and renormalization-scale dependence while the $c\bar{c}$ radius is the J/ψ radius in the attractive Coulomb potential, $r_{J/\psi} = 0.348$ fm. In Fig. 1, gluon field operators are renormalized at three scales $\epsilon_0, \sqrt{2}\epsilon_0, Q^0$, respectively. The coupling constant has the value $\alpha_s = \frac{4}{3}\sqrt{\frac{\epsilon_0}{m_c}}$ corresponding to the scale ϵ_0 while it varies for the other two scales. Values of the cross section at $\sqrt{s} = 10$ GeV are a little lower than the nucleon-J/ψ dissociation cross section obtained by the subtraction of quasi-elastic cross section in Ref. [29] from the total cross section given in Ref. [30]. In high-temperature hadronic matter or J/ψ photoproduction reaction, a typical value of the center-of-mass energy for nucleon-J/ψ (or preresonance) dissociation is around $\sqrt{s} = 6$ GeV [1]. At this energy, Fig. 2 is drawn to show the size dependence of $\sigma_{Nc\bar{c}[1^3S_1^{(1)}]}$, with $f_{g/N}(x,Q^2)$ at $Q^2 = \epsilon_0^2$.

For the S-wave color octet the nucleon-$c\bar{c}[S^{(8)}]$ cross section is

$$\sigma_{Nc\bar{c}[S^{(8)}]} = \int_{x_{min}^{(8)}}^{1} dx f_{g/N}(x, (q+Q^0)^2)\sigma_{gc\bar{c}[S^{(8)}]} \tag{20}$$

where $x_{min}^{(8)} = \frac{\Lambda_{QCD}}{p_N}$. For the P-wave color octet the nucleon-$c\bar{c}[P^{(8)}]$ cross section is

$$\sigma_{Nc\bar{c}[P^{(8)}]} = \int_{x_{min}^{(8)}}^{1} dx f_{g/N}(x, (q+Q^0)^2)\sigma_{gc\bar{c}[P^{(8)}]} \tag{21}$$

Since the gluon momentum in a confining medium is bigger than the QCD scale [14], the lowest value of x is set by $\Lambda_{QCD} = 0.2322$ GeV used in the leading order GRV parton distribution functions. Dependences of $\sigma_{Nc\bar{c}[S^{(8)}]}$ and $\sigma_{Nc\bar{c}[P^{(8)}]}$ on the center-of-mass energy $\sqrt{s}$ are depicted in Fig. 3 while the size of $(c\bar{c})_8$ is the full size of J/ψ. The dot-dashed line is obtained with the nucleon-J/ψ cross section given by Eq. (24) in Ref. [1] where another gluon distribution function evaluated at $Q^2 = \epsilon_0^2$ is used. While the $(c\bar{c})_8$ has small momentum in a nucleus, the cross section for nucleon-$(c\bar{c})_8$ production is lower than the absorption cross section determined by Gerschel and Hüfner [31] or the two-gluon exchange result [32]. It was proposed by Kharzeev and Satz that the color octet plus a gluon configuration is a dominant component produced in the proton-nucleus collisions [14]. In fact, the present cross section for a nucleon and a bare $(c\bar{c})_8$ is one part of the nucleon-$g(c\bar{c})_8$ cross section.

A $(c\bar{c})_8$ pair produced at a collision point expands before becoming color singlet to a size which may be larger or smaller than the full size of J/ψ. We then show in Fig. 4 the dependence of the nucleon-$(c\bar{c})_8$ cross section on the color-octet pair radius.

We do not want to address proton-nucleus collisions in terms of nucleon-$c\bar{c}$ cross sections [33, 34] since only the gluon-$c\bar{c}$ cross sections are needed to study $c\bar{c}$ suppression in the prethermal and thermal stages. In proton-nucleus collisions, once a color-octet $(c\bar{c})_8$ pair is produced, it picks up a collinear gluon to form a colorless configuration [14]. However, in central Au-Au collisions at RHIC and LHC energies, the accompanying gluon scatters with other hard gluons in the dense partonic system and is driven away. Therefore the bare $c\bar{c}$ is the object that we want to study in the partonic system.

6.2. J/ψ number distributions with suppression

J/ψ number distributions versus transverse momentum at $y = 0$ and rapidity at $p_T = 4$ GeV for central Au-Au collisions at RHIC energy $\sqrt{s} = 200A$GeV are calculated with respect to the initial collision, prethermal and thermal stages. Initial productions of $c\bar{c}$ are calculated with GRV parton distribution functions at renormalization scale $\mu = \sqrt{p_\perp^2 + 4m_c^2}$. Evolution of color-octet states ${}^3S_1$, ${}^1S_0$ and ${}^3P_J$ toward the J/ψ is specified by nonperturbative matrix elements $< \mathcal{O}_8^{J/\psi}({}^3S_1) >$, $< \mathcal{O}_8^{J/\psi}({}^1S_0) >$ and $< \mathcal{O}_8^{J/\psi}({}^3P_0) >$ in nonrelativistic QCD [17]. In the nonperturbative evolution, a gluon from the partonic system hits and prevents the color octet from color neutralizing via $g + (c\bar{c})_8 \to (c\bar{c})_8$. This medium effect has been expressed by exponentials in Eqs. (2), (6), (8), (10) and (11). Therefore, the nonperturbative matrix elements are assumed to be invariant while the medium effect is factorized into exponential forms. Values of these matrix elements

are well determined by fitting the CDF measurements for $p\bar{p}$ collisions at $\sqrt{s} = 1.8$ TeV in Ref. [35],

$$< \mathcal{O}_8^{J/\psi}(^3S_1) >= (1.12 \pm 0.14) \times 10^{-2}\text{GeV}^3 \tag{22}$$

$$< \mathcal{O}_8^{J/\psi}(^1S_0) > + \frac{3.5}{m_c^2} < \mathcal{O}_8^{J/\psi}(^3P_0) >= (3.90 \pm 1.14) \times 10^{-2}\text{GeV}^3 \tag{23}$$

In $p\bar{p}$ collisions, differential cross sections of direct J/ψ production depend on the combination of $< \mathcal{O}_8^{J/\psi}(^1S_0) >$ and $< \mathcal{O}_8^{J/\psi}(^3P_0) >$. However, since the dissociation cross section for the S-wave color-octet state is different from that for the P-wave color-octet state, such a dependence on the combination is destroyed. In calculations, values are taken as follows,

$$< \mathcal{O}_8^{J/\psi}(^1S_0) >= 4 \times 10^{-2}\text{GeV}^3, \quad < \mathcal{O}_8^{J/\psi}(^3P_0) >= -\frac{m_c^2}{35} \times 10^{-2}\text{GeV}^3 \tag{24}$$

The value of $< \mathcal{O}_8^{J/\psi}(^3P_0) >$ is positive at tree level and negative after renormalization [36]. Eq. (23) is still satisfied by the values in Eq. (24). These values of nonperturbative matrix elements are supposed to be universal for any center-of-mass energy $\sqrt{s}$.

Various contributions to the J/ψ number distributions including initial collisions, prethermal and thermal stages, $2 \to 1$ and $2 \to 2$ collisions, are drawn separately in Figs. 5 and 6. The dashed curve resulting from $c\bar{c}$ production in the initial collision is obtained by calculating Eq. (2) where the nuclear parton shadowing factor is given in Ref. [4] throughout this subsection. The upper and lower dot-dashed curves resulting from $c\bar{c}$ production in the prethermal stage are obtained by individually calculating Eq. (6) for $2 \to 1$ collisions and Eq. (8) for $2 \to 2$ collisions. The upper and lower dotted curves resulting from $c\bar{c}$ production in the thermal stage are obtained by calculating Eq. (10) for $2 \to 1$ collisions and Eq. (11) for $2 \to 2$ collisions, respectively. To exclude the effect of intrinsic transverse momentum smearing, only the region $p_T > 2$ GeV is considered. Consequently, no $2 \to 1$ collisions contribute in the initial collision. The J/ψ number distribution resulting from the initial collision shown by the dashed line has a plateau similar to that in proton-proton collision [37]. Both Figs. 5 and 6 show that $c\bar{c}$ pairs produced from the thermal stage can be neglected compared to the initial production, but the contributions from the prethermal stage are important in the transverse momentum region $2\text{GeV} < p_T < 8\text{GeV}$ and rapidity region $0 < y < 1.2$. Productions of $c\bar{c}$ in the prethermal and thermal stages bulge up the J/ψ number distribution shown by the solid line in this rapidity region. Nevertheless, the dot-dashed and dotted lines fall rapidly as the rapidity gets large. This bulging characterizes the formation of a deconfined medium because the medium has average momentum limited but big enough to produce extra $c\bar{c}$ and thus J/ψ. The $2 \to 1$ collisions in the partonic system have bigger contributions than the $2 \to 2$ collisions.

Each of Figs. 7 and 8 contains two sets of lines to show contributions from the color-singlet and color-octet pairs produced at short distance. Any set has a dashed line obtained from Eq. (2) for the initial collision, a dot-dashed line from Eq. (9) for the prethermal stage and a dotted line from Eq. (12) for the thermal stage, respectively. A line in the upper (lower) set for the color-octet (color-singlet) contributions stems from the terms for $(c\bar{c})_8$ ($(c\bar{c})_1$) states. The color octet states dominate productions of J/ψ at RHIC energy. However, the ratio of color-octet to color-singlet contributions shown by the

two solid lines at $p_T = 6$ GeV is reduced from about 70 at CDF collider energy $\sqrt{s} = 1.8$ TeV to about 40 at RHIC energy. Both contributions of color-singlet and color-octet states have similar dependence on transverse momentum and rapidity.

Figs. 9 and 10 show transverse momentum and rapidity dependence of J/ψ number distributions for central Au-Au collisions at LHC energy $\sqrt{s} = 5.5A$TeV. A prominent feature is that the J/ψ number produced from the thermal stage is comparable to that from the prethermal stage. Compared to the initial production, $c\bar{c}$ and J/ψ produced through $2 \to 2$ reactions may be neglected. A bulge is observed on the plateau in the rapidity region $0 < y < 1.5$. Such a bulge can be taken as a signature for the existence of a parton plasma at the LHC energy. Figs. 11 and 12 depict contributions from the color singlet and color octet at LHC energy. The ratio of color-octet to color-singlet contributions shown by the two solid lines at $p_T = 6$GeV reaches about 150. This indicates the color octet states become more important with the increase of $\sqrt{s}$.

6.3. Ratios including J/ψ survival probability

Nuclear shadowing results in a modification of gluon distribution functions inside a nucleus [38] and such a nuclear effect is represented by the shadowing factor $S_{a/A}$ in Eq. (3). If the $S_{a/A} = 1$ for no shadowing, the $dN^{2\to2}_{ini}/dyd^2p_\perp$ is proportional to the product of atomic masses of the two colliding nuclei. If $S_{a/A} \neq 1$ and depends on the longitudinal momentum fraction x, the production of $c\bar{c}$ is reduced in the shadowing region and enhanced for the anti-shadowing region. Irrespective of interactions of J/ψ with the partonic system, J/ψ number distributions produced in the initial central A+B collision is obtained by putting all exponentials equal to 1 in Eq. (2),

$$\begin{aligned}
\frac{dN^{2\to2}_0}{dyd^2p_\perp}(S_{a/A}) &= 2\int_{-\ln\frac{\sqrt{s}-m_\perp e^{-y}}{p_\perp}}^{\ln\frac{\sqrt{s}-m_\perp e^{y}}{p_\perp}} dy_{\rm x}\int_0^{R_A} drr \\
&\sum x_a f_{a/A}(x_a, m_\perp^2, \vec{r}) x_b f_{b/B}(x_b, m_\perp^2, -\vec{r}) \\
&\{\frac{d\sigma}{dt}(ab \to c\bar{c}[^3S_1^{(1)}]{\rm x} \to J/\psi) \\
&+\frac{d\sigma}{dt}(ab \to c\bar{c}[^3S_1^{(8)}]{\rm x} \to J/\psi) \\
&+\frac{d\sigma}{dt}(ab \to c\bar{c}[^1S_0^{(8)}]{\rm x} \to J/\psi) \\
&+\frac{d\sigma}{dt}(ab \to c\bar{c}[^3P_J^{(8)}]{\rm x} \to J/\psi)\}
\end{aligned} \tag{25}$$

To characterize the influence of nuclear parton shadowing on the J/ψ production from the initial collision, a ratio is defined as

$$R^{ini} = \frac{dN^{2\to2}_0}{dyd^2p_\perp}(S_{a/A} \neq 1)/\frac{dN^{2\to2}_0}{dyd^2p_\perp}(S_{a/A} = 1) \tag{26}$$

Here the $S_{a/A} \neq 1$ from Ref. [4] applies throughout this subsection.

The initially produced J/ψ originates from the $c\bar{c}$ pairs produced in the initial collision. Its dependence on the transverse momentum and rapidity is obtained by calculating

Eq. (25). Some $c\bar{c}$ pairs produced in the initial collision may dissociate by gluons from the partonic system. As a consequence, the J/ψ number is reduced. The survival probability for the $c\bar{c}$ transiting into a J/ψ is defined as the ratio

$$S^{plasma} = \frac{dN_{ini}^{2\to 2}}{dyd^2p_\perp}(S_{a/A} \neq 1)/\frac{dN_0^{2\to 2}}{dyd^2p_\perp}(S_{a/A} \neq 1) \tag{27}$$

We have calculated the J/ψ number distributions produced in the prethermal and thermal stages in Subsection 6.2. The J/ψ yield may be bigger than the reduced amount of initially produced J/ψ due to the $c\bar{c}$ dissociation by gluons in the partonic system. The partonic system has two roles. One is to produce $c\bar{c}$ pairs and another is to dissociate $c\bar{c}$ pairs. To see the roles, a ratio is defined by

$$R^{plasma} = (\frac{dN_{ini}^{2\to 2}}{dyd^2p_\perp}(S_{a/A} \neq 1) + \frac{dN_{pre}}{dyd^2p_\perp} + \frac{dN_{the}}{dyd^2p_\perp})/\frac{dN_0^{2\to 2}}{dyd^2p_\perp}(S_{a/A} \neq 1) \tag{28}$$

To understand the nuclear effect on parton distributions and the roles of the partonic system, we need to compare J/ψ production in the central A+B collision with that in the nucleon-nucleon collision. To this end, a ratio is defined as

$$R = (\frac{dN_{ini}^{2\to 2}}{dyd^2p_\perp}(S_{a/A} \neq 1) + \frac{dN_{pre}}{dyd^2p_\perp} + \frac{dN_{the}}{dyd^2p_\perp})/\frac{dN_0^{2\to 2}}{dyd^2p_\perp}(S_{a/A} = 1) \tag{29}$$

which is also written as

$$R = R^{ini}R^{plasma} \tag{30}$$

The ratios R^{ini}, S^{plasma}, R^{plasma} and R versus transverse momentum and rapidity are depicted as dashed, dotted, dot-dashed and solid lines, respectively, in Figs. 13 and 14 for the RHIC energy and Figs. 15 and 16 for the LHC energy. In contrast to $R^{ini} < 1$, the value of R^{plasma} is larger than 1 for all transverse momenta in Fig. 13 and $0 < y < 1.5$ in Fig. 14 and $0.5 < y < 1.5$ in Fig. 16. This results in prominent bulges on the solid lines of R in Figs. 14 and 16. In contrast, the survival probability S^{plasma} shown by the dotted lines has no such bulge. Therefore, the bulges are present in Figs. 6 and 10 when the J/ψ yield resulting from $c\bar{c}$ pairs produced in the partonic system overwhelms the reduced amount of initially produced J/ψ. We conclude that in the rapidity region $0 < y < 1.5$ a bulge observed in the ratio R is an indicator for the existence of the partonic system. For $R^{ini} < 1$ and $S^{plasma} < 1$, J/ψ suppression arises from the nuclear parton shadowing found in HIJING and $c\bar{c}$ dissociation in the partonic system.

6.4. J/ψ number distributions with no suppression

In Subsection 6.2, J/ψ number distributions have been presented while the $c\bar{c}$ reduction due to the nuclear parton shadowing in the initial collision and $c\bar{c}$ dissociation in the partonic system are taken into account. In this subsection, the suppression including both the reduction and dissociation is omitted in calculations of J/ψ number distributions by setting to 1 all exponentials in Eqs. (2), (6), (8), (10) and (11). Figs. 17-20 depict these distributions versus transverse momentum at $y = 0$ and rapidity at $p_T = 4$ GeV at both RHIC and LHC energies. We are now ready to explain the dip within $y < 1$ in Fig. 10. This dip disappears in Fig. 20 where suppression is not considered. Since R^{ini} shown

by the dashed line in Fig. 16 is flat with respect to the rapidity $y < 2$ and S^{plasma} shown by the dotted line has a steep rise in $0.5 < y < 1$, the dip phenomenon is solely due to the $c\bar{c}$ dissociation in the partonic system. Such a dip phenomenon is not obvious but still can be observed in the prethermal and thermal stages when the J/ψ number distributions with suppression are compared to those without suppression. The comparison is indicated in Fig. 21 for the prethermal stage and Fig. 22 for the thermal stage. The solid and dot-dashed lines for no suppression begin to fall from $y = 0.5$ to $y = 1$, but change to rising as shown by the dashed and dotted lines when the $c\bar{c}$ dissociation is switched on. This change occurs because of the steep rise of S^{plasma}. A relatively weak dependence of S^{plasma} on p_T is shown by the dotted line in Fig. 15. The dip phenomenon thus cannot be observed in the p_T dependence of J/ψ number distributions. Referring back to Eqs. (2), (6), (8), (10) and (11), exponentials there have sensitive dependence on the rapidity in $0 < y < 1.5$. The dip is more obvious in the color singlet channel as shown by the lower solid, dashed, dot-dashed and dotted lines in Fig. 12. This is so because the cross section for the $1^3S_1^{(1)}$-state dissociation has a narrower peak with respect to the incident gluon energy [12] than the color octet states.

6.5. Uncertainties

Since gluon shadowing in nuclei has not been studied experimentally, theoretical estimates of the nuclear gluon shadowing factor involve uncertainties. The nuclear parton shadowing factor found in HIJING [4] is a result of the assumption that there is no Q-dependence on the shadowing factor and the shadowing effect for gluons and quarks is the same. Nevertheless, the shadowing factor has been shown by Eskola *et al.* to evolve with momentum Q [39]. The difference between the latter and the former indicates uncertainty. The ratio R^{ini} defined in Eq. (26) is calculated with Eskola *et al.*'s parametrization [39] and results are depicted in Fig. 23 showing momentum dependence at $y = 0$ and Fig. 24 showing rapidity dependence at $p_T = 4$ GeV. Compared to the dashed lines in Figs. 13-16, the change of R^{ini} at RHIC energy greater than 1 is prominent. This implies that the anti-shadowing effect of Eskola *et al.*'s parametrization is quite important at RHIC energy. Measurements on R^{ini} in RHIC experiments are needed to confirm this nuclear enhancement [21].

The ratio R^{ini} is always flat within the rapidity region $-1.5 < y < 1.5$ for parametrizations given in HIJING and by Eskola *et al.*, and the flatness seems to be independent of parametrizations. If the partonic system does not come into being, the ratio R is flat, too, since $R = R^{ini}$. If the partonic system dissociates $c\bar{c}$ pairs, the solid curve of R undergoes bulging, dipping and then bulging from $y = -1.5$ to $y = 1.5$. Any such twist of R in $-1.5 < y < 1.5$ observed in experiments is nontrivial, because only a deconfined medium generates it.

Upon inclusion of uncertainties on the formation and evolution of parton plasma arising from other factors, for instance, the dependence on the coupling constant α_s [40] and transverse flow [41], the J/ψ number distribution and the four ratios including survival probability will change. In the partonic system considered here gluons dominate the evolution and gluon-$c\bar{c}$ interactions break the pairs. In a system where quarks and antiquarks are abundant, interactions between quarks (antiquarks) and $c\bar{c}$ may account for a suppression of J/ψ [42]. Additional suppression caused by energy loss of the initial

state has not been considered since there is a controversy on the influence of the energy loss [43, 44]. Some uncertainties are expected to be fixed by upcoming experiments at RHIC.

7. Conclusions

We have studied J/ψ production through both color-singlet and color-octet $c\bar{c}$ channels with various stages of central Au-Au collisions at both RHIC and LHC energies. In addition to the scattering processes $ab \to c\bar{c}[^{2S+1}L_J]$x, contributions of the reactions $ab \to c\bar{c}[^{2S+1}L_J]$ are also calculated in the prethermal stage and thermal stage. The effect of the medium on an expanding $c\bar{c}$ involves a gluon interacting with the $c\bar{c}$ to prevent it from a transition into a color singlet. Cross sections for $g + c\bar{c} \to (c\bar{c})_8$ are calculated with internal wave functions of $(c\bar{c})_1$ in an attractive potential and $(c\bar{c})_8$ in a repulsive potential. Furthermore, nucleon-$c\bar{c}$ cross sections for color singlet, S- and P- wave color octets as a function of $\sqrt{s}$ or $c\bar{c}$ radius are evaluated by assuming that the nucleon dominantly contains gluons. Momentum and rapidity dependence of J/ψ number distribution with various contributions are calculated for central Au-Au collisions at both RHIC and LHC energies. Color octet contributions are one order of magnitude larger than the color singlet contributions. Yields of $c\bar{c}$ are large in the prethermal stage at RHIC energy and through the $2 \to 1$ collisions $ab \to c\bar{c}[^{2S+1}L_J]$ at LHC energy. Since the partonic system offers fairly large amounts of $c\bar{c}$, a bulge in $0 < y < 1.5$ at RHIC energy and $0.5 < y < 1.5$ at LHC energy can be observed in the rapidity dependence of the J/ψ number distribution and the ratio R of J/ψ number distributions for Au-Au collisions to nucleon-nucleon collisions. Such a bulge is a signature for the existence of a deconfined partonic medium. We suggest that RHIC and LHC experiments measure J/ψ number distributions and the ratio R in the rapidity region $0 < y < 3$ to observe a bulge. While the yield of $c\bar{c}$ from the medium is larger than the reduced amount of initial production in the medium, the ratio R^{plasma} is larger than 1. The competition between production and suppression determines the values of R^{plasma}, which relies on the evolution of parton number density and temperature of the partonic system [12]. A dip in the rapidity dependence of the J/ψ number distributions at LHC energy may exist and this amounts to a suppression effect of $c\bar{c}$ in the partonic system. So far, we have obtained results and conclusions for positive rapidity. It is stressed that the same contents for negative rapidity can be obtained from the positive region by symmetry.

Acknowledgements

I thank the [Department of Energy's] Institute for Nuclear Theory at the University of Washington for its hospitality and the Department of Energy for partial support during the completion of this work. I thank the Nuclear Theory Group at LBNL Berkeley for their hospitality during my visit. I also thank X.-N. Wang, C.-Y. Wong and M. Asakawa for discussions, K. J. Eskola for offering Fortran codes of nuclear parton shadowing factors, H. J. Weber for careful reading through the manuscript. This work was also supported in part by the project KJ951-A1-410 of the Chinese Academy of Sciences and the Education Bureau of Chinese Academy of Sciences.

References

[1]D. Kharzeev and H. Satz, Phys. Lett. B334(1994)155.

[2]R. C. Hwa and K. Kajantie, Phys. Rev. Lett. 56(1986)696;
J. P. Blaizot and A. H. Mueller, Nucl. Phys. B289(1987)847.

[3]K. Kajantie, P. V. Landshoff, and J. Lindfors, Phys. Rev. Lett. 59 (1987)2517;
K. J. Eskola, K. Kajantie, and J. Lindfors, Nucl. Phys. B323(1989)37;
Phys. Lett. B214(1991)613.

[4]X.-N. Wang and M. Gyulassy, Phys. Rev. D44(1991)3501; Comput. Phys. Commun. 83(1994)307.
X.-N. Wang, Phys. Rep. 280(1997)287.

[5]K. Geiger and B. Müller, Nucl. Phys. B369(1992)600;
K. Geiger, Phys. Rev. D47(1993)133.

[6]H. J. Moehring and J. Ranft, Z. Phys. C52(1991)643;
P. Aurenche et al., Phys. Rev. D45(1992)92;
P. Aurenche et al., Comput. Phys. Commun. 83(1994)107.

[7]E. Shuryak, Phys. Rev. Lett. 68(1992)3270;
L. Xiong and E.Shuryak, Phys. Rev. C49(1994)2203.

[8]K. Geiger and J. I. Kapusta, Phys. Rev. D47(1993)4905.

[9]T. S. Biró, E. van Doorn, B. Müller, M. H. Thoma, and X.-N. Wang, Phys. Rev. C48(1993)1275.

[10]J. Alam, S. Raha and B. Sinha, Phys. Rev. Lett. 73(1994)1895.

[11]H. Heiselberg and X.-N. Wang, Phys. Rev. C53(1996)1892.

[12]X.-M. Xu, D. Kharzeev, H. Satz and X.-N. Wang, Phys. Rev. C53 (1996)3051.

[13]T. Matsui and H. Satz, Phys. Lett. B178(1986)416.

[14]D. Kharzeev and H. Satz, Phys. Lett. B366(1996)316.

[15]D. M. Alde et al., Phys. Rev. Lett. 66(1991)133;
D. M. Alde et al., Phys. Rev. Lett. 66(1991)2285;
L. Antoniazzi et al., Phys. Rev. Lett. 70(1993)383;
M. H. Schub et al., Phys. Rev. D52(1995)1307;
T. Alexopoulos et al., Phys. Rev. D55(1997)3927

[16]F. Abe et al., CDF Collaboration, Phys. Rev. Lett. 79(1997)572,578

[17]W. E. Caswell and G. P. Lepage, Phys. Lett. B167(1986)437;
G. P. Lepage, L. Magnea, C. Nakhleh, U. Magnea and K. Hornbostel, Phys. Rev. D46(1992)4052;
G. T. Bodwin, E. Braaten and G. P. Lepage, Phys. Rev. D51(1995)1125.

[18]P. Lévai, B. Müller and X.-N. Wang, Phys. Rev. C51(1995)3326.

[19]Z. Lin and M. Gyulassy, Phys. Rev. C51(1995)2177.

[20]K. J. Eskola and X.-N. Wang, Phys. Rev. D49(1994)1284.

[21]Y. Akiba, in Proc. of Charmonium Production in Relativistic Nuclear Collisions, INT, Seattle, 1998, eds. B. Jacak and X.-N. Wang (World Scientific, Singapore,1998);
M. Rosati, in Proc. of Charmonium Production in Relativistic Nuclear Collisions, INT, Seattle, 1998, eds. B. Jacak and X.-N. Wang (World

Scientific, Singapore,1998)
[22]S. Gupta and H. Satz, Z. Phys. C55(1992)391.
R. C. Hwa and L. Leśniak, Phys. Lett. B295(1992)11.
R. Vogt, S. J. Brodsky and P. Hoyer, Nucl Phys. B360(1991)67;
K. Boreskov, A. Capella, A. Kaidalov and J. Tran Thanh Van, Phys. Rev. D47(1993)919.
M. A. Braun, C. Pajares, C. A. Salgado, N. Armesto and A. Capella, Nucl. Phys. B509(1998)357.
[23]P. Cho and A. K. Leibovich, Phys. Rev. D53(1996)150,6203.
[24]K. Sridhar, A. D. Martin and W. J. Stirling, Phys. Lett. B438(1998)211.
[25]R. Baier and R. Rückl, Z. Phys. C19(1983)251;
R. Gastmans, W. Troost and T. T. Wu, Nucl. Phys. B291(1987)731.
[26]M. E. Peskin, Nucl. Phys. B156(1979)365;
G. Bhanot and M. E. Peskin, Nucl. Phys. B156(1979)391.
[27]B. Z. Kopeliovich and B. G. Zakharov, Phys. Rev. D44(1991)3466;
L. Frankfurt, G. A. Miller and M. Strikman, Phys. Lett. B304(1993)1;
L. Gerland, L. Frankfurt, M. Strikman, H. Stöcker and W. Greiner, Phys. Rev. Lett. 81(1998)762.
P. Jain, B. Pire and J. P. Ralston, Phys. Rep. 271(1996)67.
[28]M. Glück, E. Reya and A. Vogt, Z. Phys. C67(1995)433.
[29]R. L. Anderson, SLAC-Pub 1741(1976).
[30]J. Hüfner and B. Z. Kopeliovich, Phys. Lett. B426(1998)154.
[31]C. Gerschel and J. Hüfner, Z. Phys. C56(1992)171.
[32]J. Dolejši and J. Hüfner, Z. Phys. C54(1992)489.
C. W. Wong, Phys. Rev. D54(1996)R4199.
[33]C.-Y. Wong and C. W. Wong, Phys. Rev. D57(1998)1838.
[34]W. Cassing and E. L. Bratkovskaya, Nucl. Phys. A623(1997)570.
[35]M. Beneke and M. Krämer, Phys. Rev. D55(1997)R5269.
[36]J. Amundson, S. Fleming and I. Maksymyk, Phys. Rev. D56(1997)5844;
T. Mehen, Phys. Rev. D55(1997)4338.
[37]R. Gavai et al., Int. J. Mod. Phys. A10(1995)3043.
[38]A. H. Mueller and J. Qiu, Nucl. Phys. B268(1986)427;
K. J. Eskola, J. Qiu and X.-N. Wang, Phys. Rev. Lett. 72(1994)36;
M. Arneodo, Phys. Rep. 240(1994)301.
[39]K. J. Eskola, V. J. Kolhinen and C. A. Salgado, JYFL-8/98, US-FT/14-98, hep-ph/9807297.
K. J. Eskola, V. J. Kolhinen and P. V. Ruuskanen, CERN-TH/97-345, JYFL-2/98, hep-ph/9802350.
[40]S. M. H. Wong, Phys. Rev. C56(1997)1075.
[41]D. K. Srivastava, M. G. Mustafa and B. Müller, Phys. Rev. C56(1997)1064.
[42]R. Wittmann and U. Heinz, Z. Phys. C59(1993)77.
[43]S. Gavin and J. Milana, Phys. Rev. Lett. 68(1992)1834;
E. Quack and T. Kodama, Phys. Lett. B302(1993)495;
R. C. Hwa, J. Pišút and N. Pišútová, Phys. Rev. C56(1997)432.
[44]S. J. Brodsky and P. Hoyer, Phys. Lett. B298(1993)165.

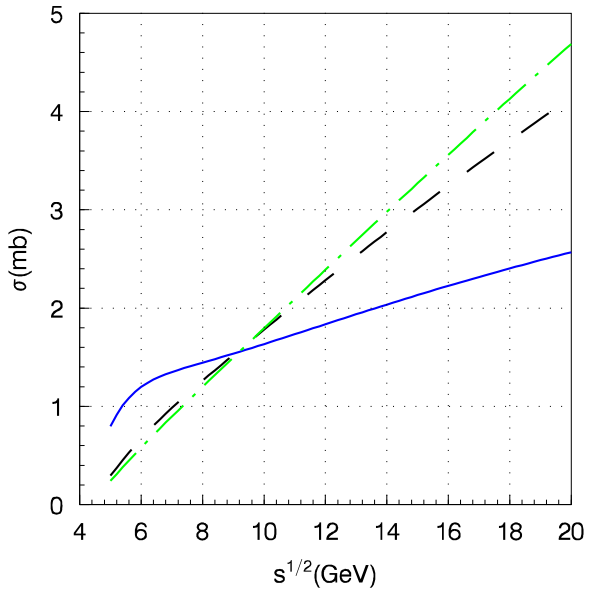

Figure 1: Solid, dashed and dot-dashed lines are nucleon-$c\bar{c}[1^3S_1^{(1)}]$ cross sections for $f_{g/N}(x,Q^2)$ evaluated at $Q^2=\epsilon_0^2, 2\epsilon_0^2, (Q^0)^2$, respectively. The $(c\bar{c})_1$ has the same size as J/ψ.

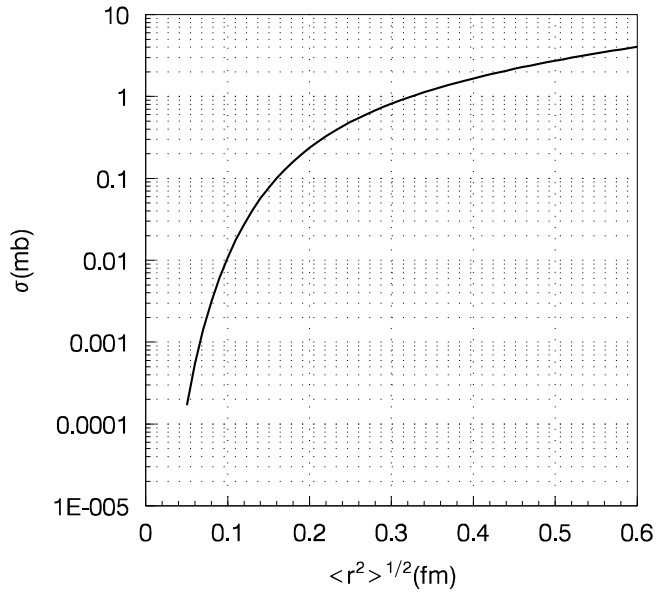

Figure 2: Cross section for nucleon-$c\bar{c}[1^3S_1^{(1)}]$ at $\sqrt{s}=6$ GeV as a function of the $c\bar{c}$ radius is calculated with $f_{g/N}(x,Q^2)$ evaluated at $Q^2=\epsilon_0^2$.

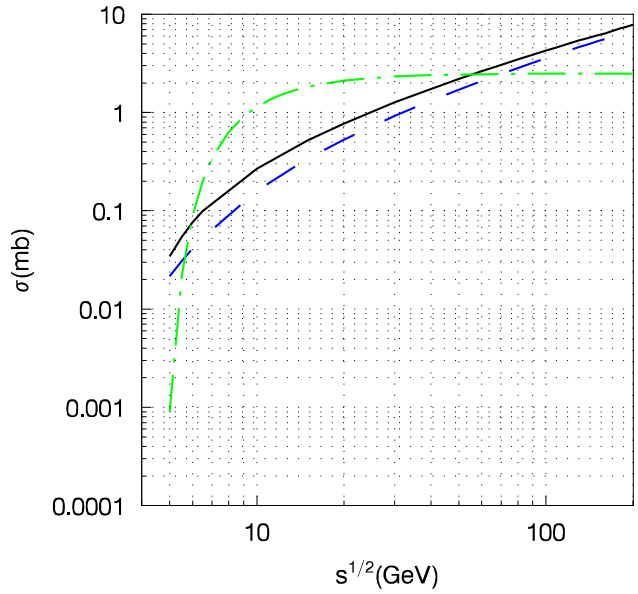

Figure 3: The solid and dashed lines are cross sections for nucleon-$c\bar{c}[S^{(8)}]$ and nucleon-$c\bar{c}[P^{(8)}]$ collisions as a function of $\sqrt{s}$, respectively. The dot-dashed line is the nucleon-J/ψ cross section calculated with Eq. (24) in Ref. [1]. The corresponding $(c\bar{c})_8$ and J/ψ have the same radius.

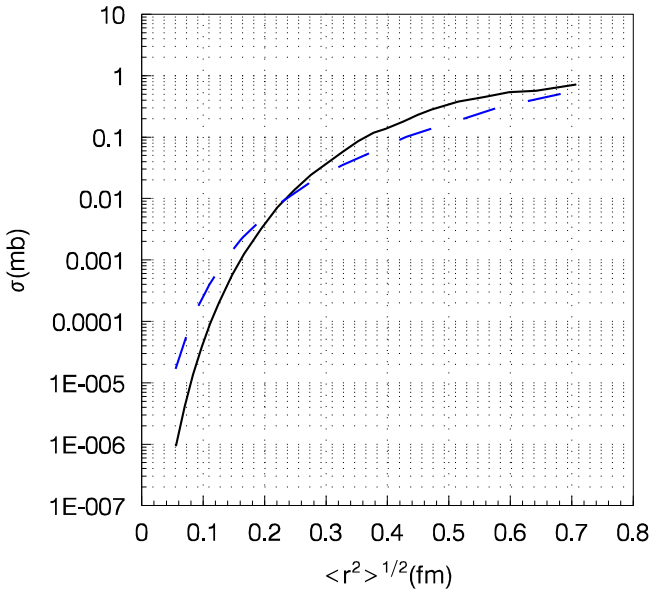

Figure 4: The solid and dashed lines show radius dependence of cross sections for nucleon-$(c\bar{c})_8[S^{(8)}]$ and nucleon-$(c\bar{c})_8[P^{(8)}]$ collisions, respectively.

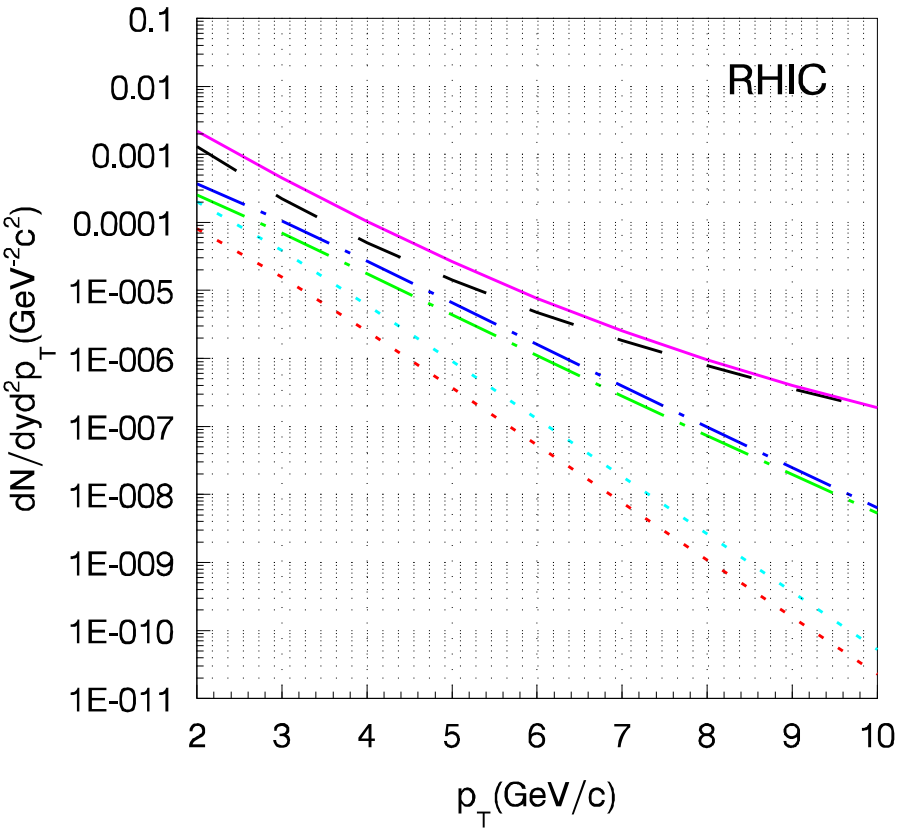

Figure 5: J/ψ number distributions versus transverse momentum at $y = 0$ and RHIC energy with suppression. The dashed curve corresponds to $c\bar{c}$ production in the initial collision. The upper and lower dot-dashed (dotted) curves correspond to $c\bar{c}$ produced through $2 \to 1$ and $2 \to 2$ reactions in the prethermal (thermal) stage, respectively. The solid curve is the sum of all contributions.

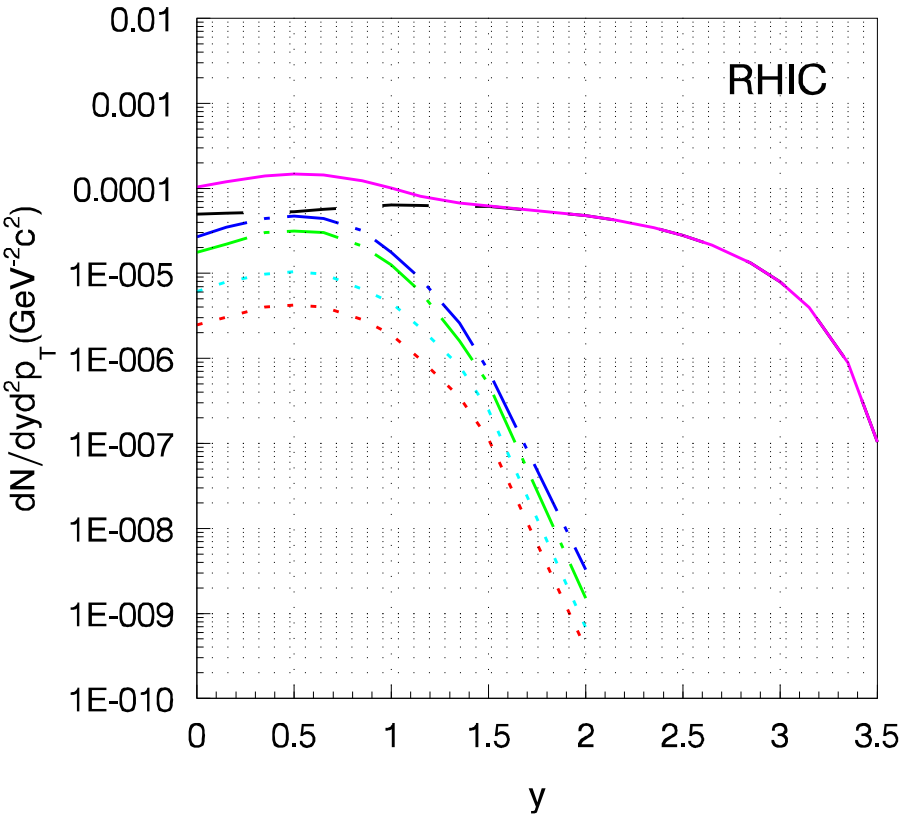

Figure 6: The same as Fig. 5, except for rapidity distribution at $p_T = 4$ GeV.

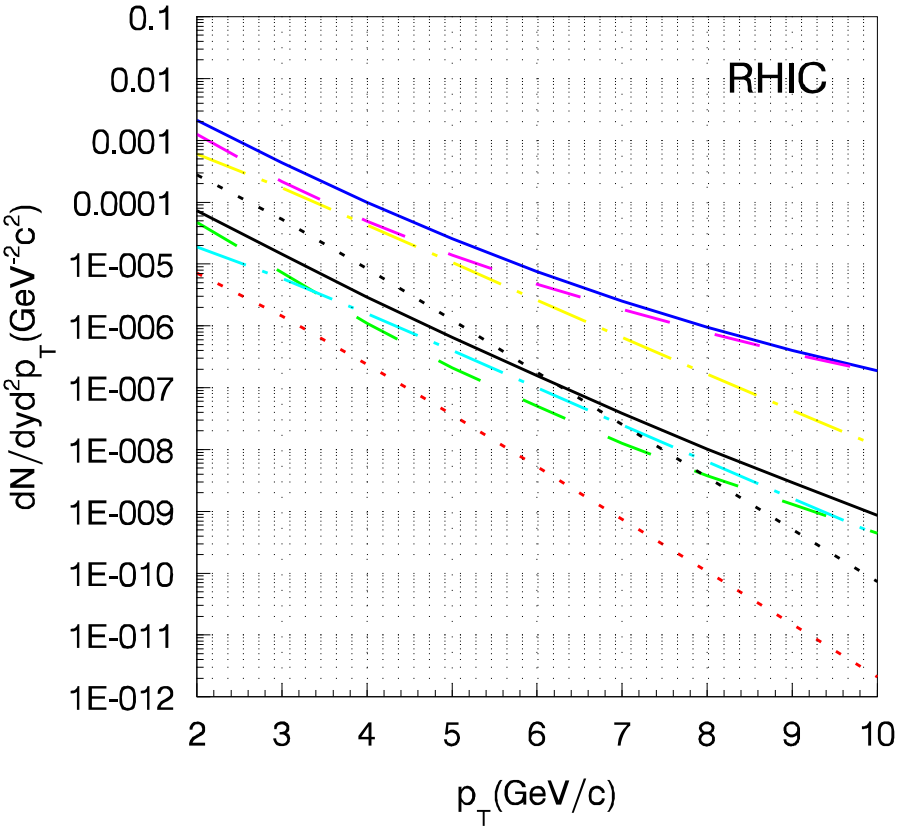

Figure 7: J/ψ number distributions versus transverse momentum at $y = 0$ and RHIC energy with suppression. The upper and lower dashed (dot-dashed, dotted and solid) lines correspond to $c\bar{c}$ in color octet and color singlet, respectively, produced in the initial collision(prethermal stage, thermal stage and the all three stages).

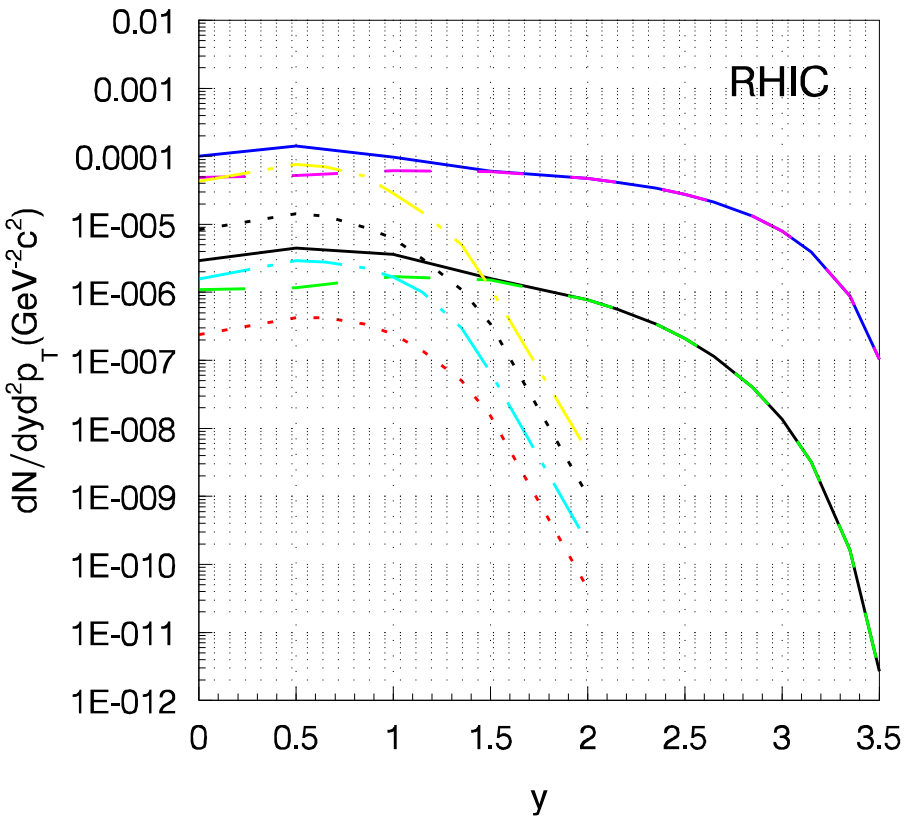

Figure 8: The same as Fig. 7, except for rapidity distribution at $p_T = 4$ GeV.

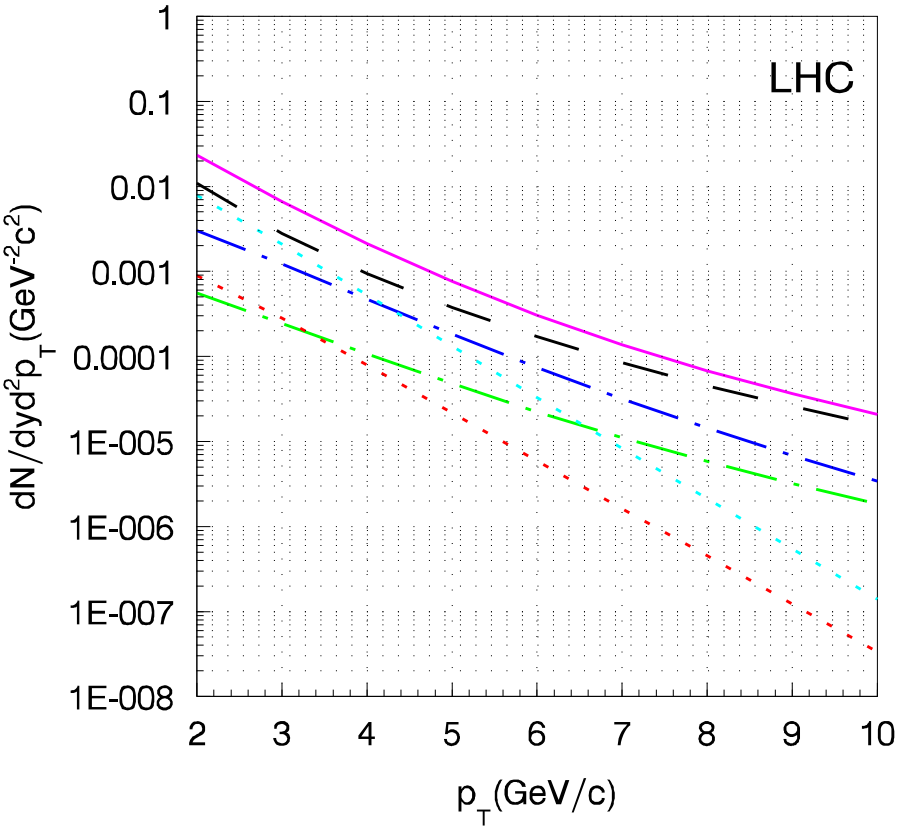

Figure 9: J/ψ number distributions versus transverse momentum at $y = 0$ and LHC energy with suppression. The dashed curve corresponds to $c\bar{c}$ productions in the initial collision. The upper and lower dot-dashed (dotted) curves correspond to $c\bar{c}$ produced through $2 \to 1$ and $2 \to 2$ reactions in the prethermal (thermal) stage, respectively. The solid curve is the sum of all contributions.

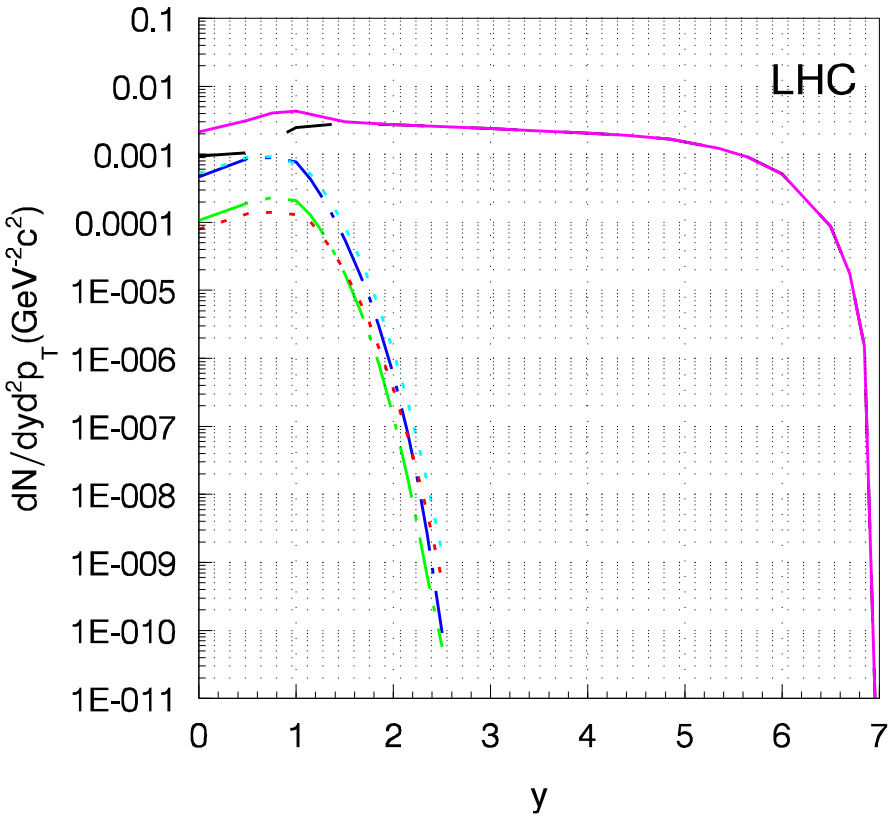

Figure 10: The same as Fig. 9, except for rapidity distribution at $p_T = 4$ GeV.

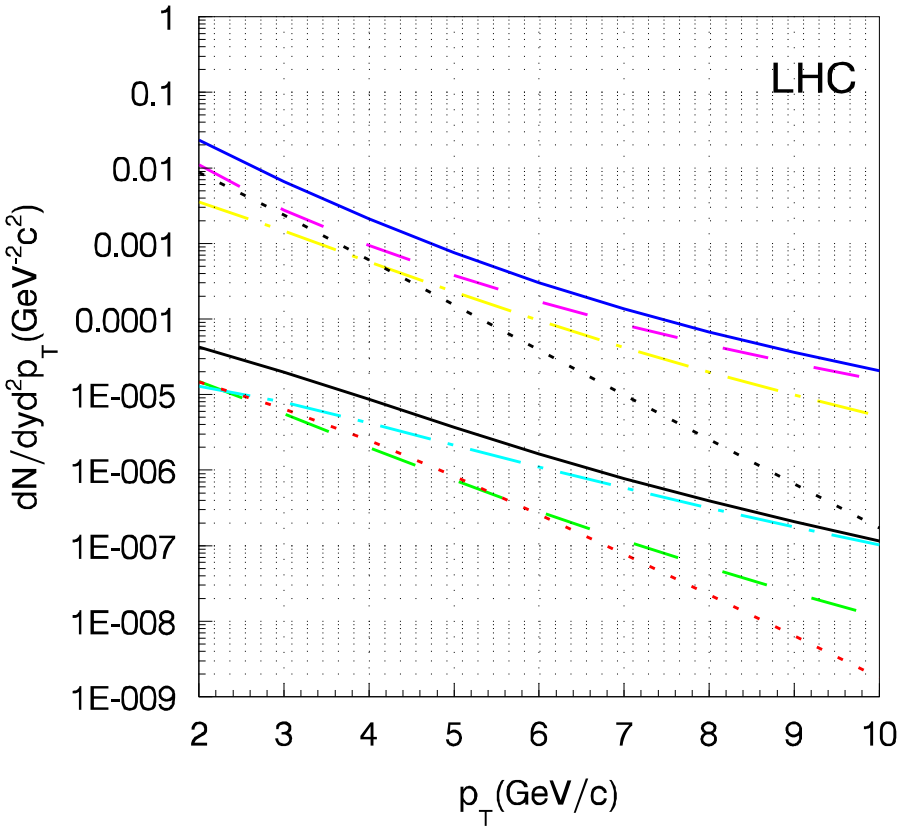

Figure 11: J/ψ number distributions versus transverse momentum at $y = 0$ and LHC energy with suppression. The upper and lower dashed (dot-dashed, dotted and solid) lines correspond to $c\bar{c}$ in color octet and color singlet, respectively, produced in the initial collision (prethermal stage, thermal stage and all three stages).

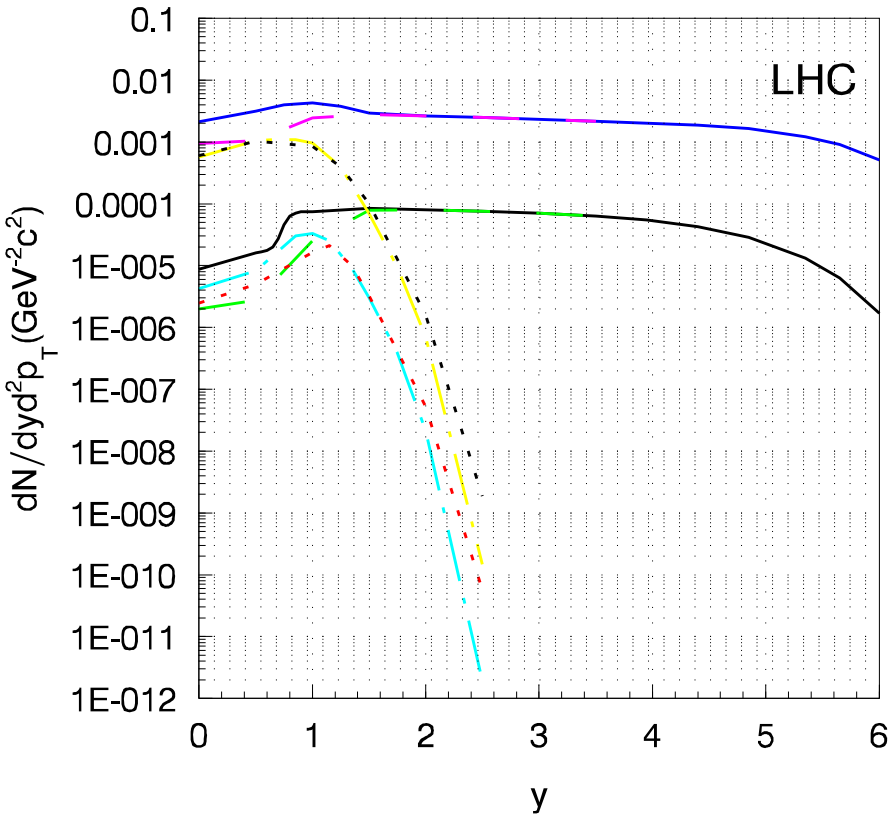

Figure 12: The same as Fig. 11, except for rapidity distribution at $p_T = 4$ GeV.

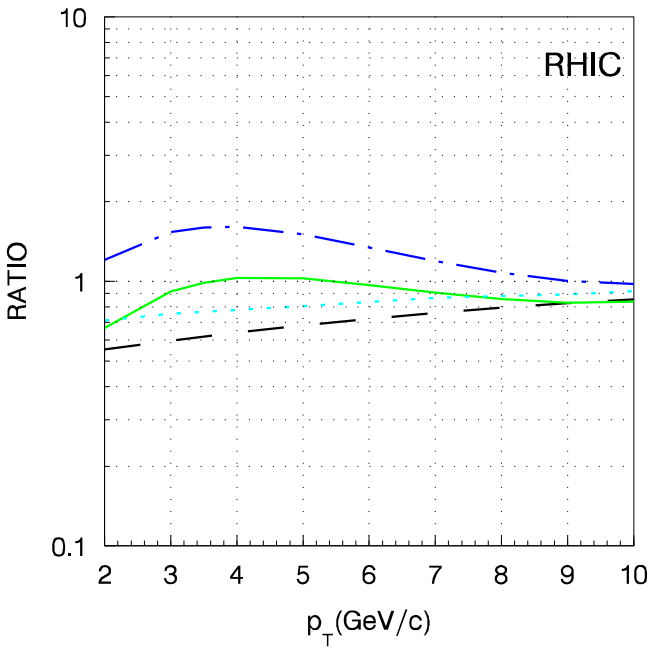

Figure 13: Ratios versus transverse momentum at $y = 0$ and RHIC energy. The solid, dashed, dot-dashed and dotted lines are R, R^{ini}, R^{plasma} and S^{plasma}, respectively.

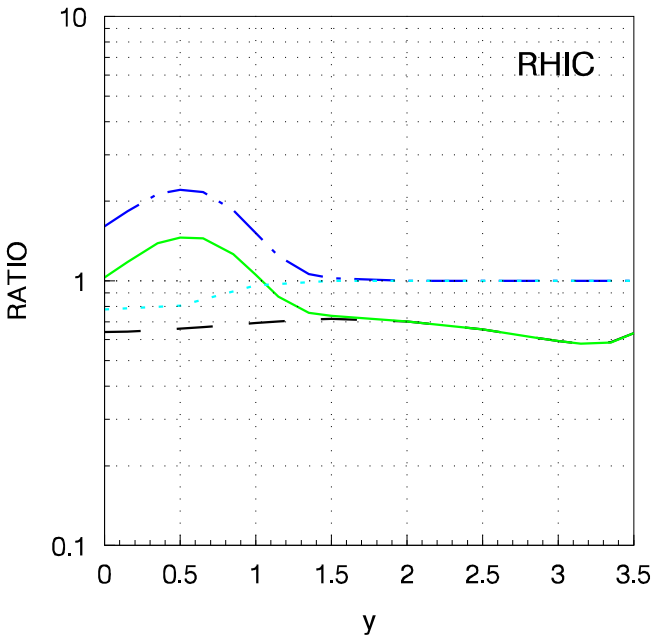

Figure 14: The same as Fig. 13, except for rapidity distribution at $p_T = 4$ GeV

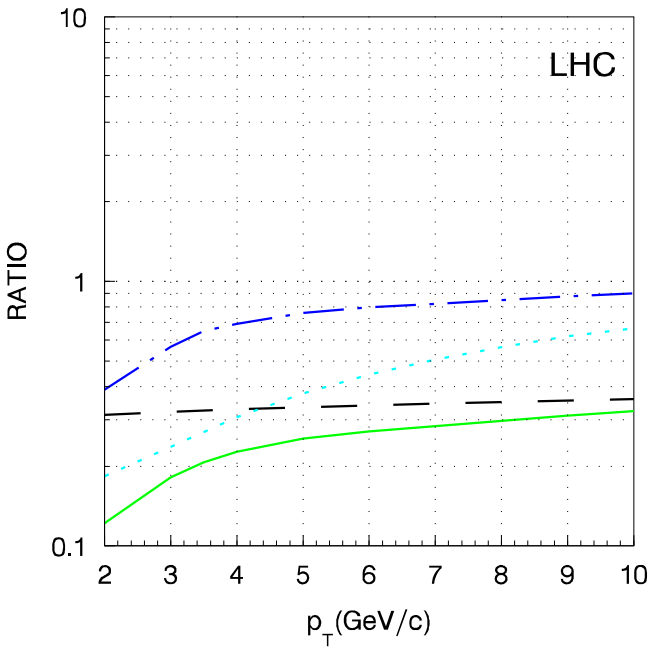

Figure 15: Ratios versus transverse momentum at $y = 0$ and LHC energy. The solid, dashed, dot-dashed and dotted lines are R, R^{ini}, R^{plasma} and S^{plasma}, respectively.

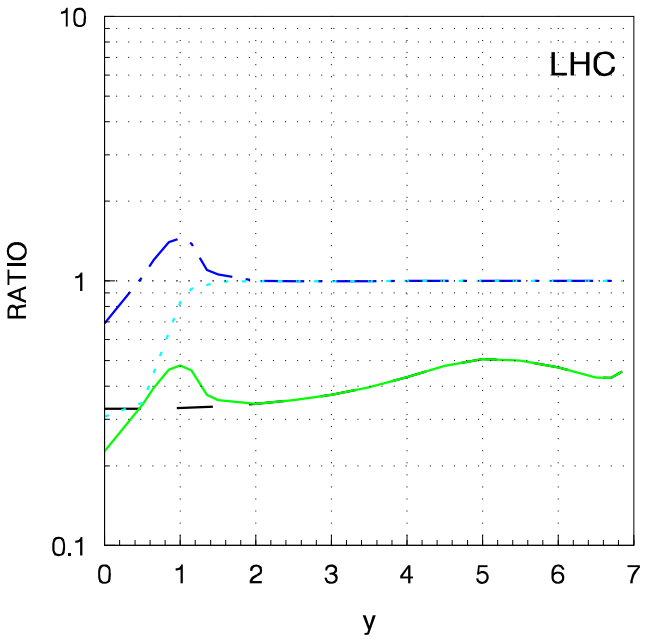

Figure 16: The same as Fig. 15, except for rapidity distribution at $p_T = 4$ GeV.

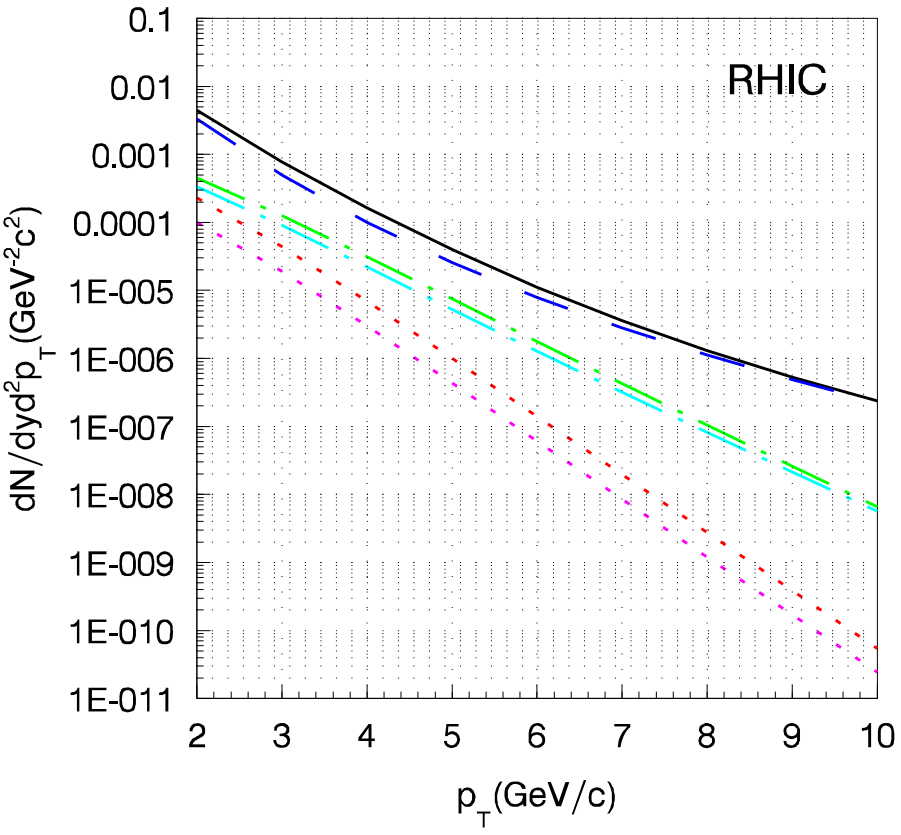

Figure 17: J/ψ number distributions versus transverse momentum at $y = 0$ and RHIC energy without suppression. The dashed curve corresponds to $c\bar{c}$ productions in the initial collision. The upper and lower dot-dashed (dotted) curves correspond to $c\bar{c}$ produced through $2 \to 1$ and $2 \to 2$ reactions in the prethermal (thermal) stage, respectively. The solid curve is the sum of all contributions.

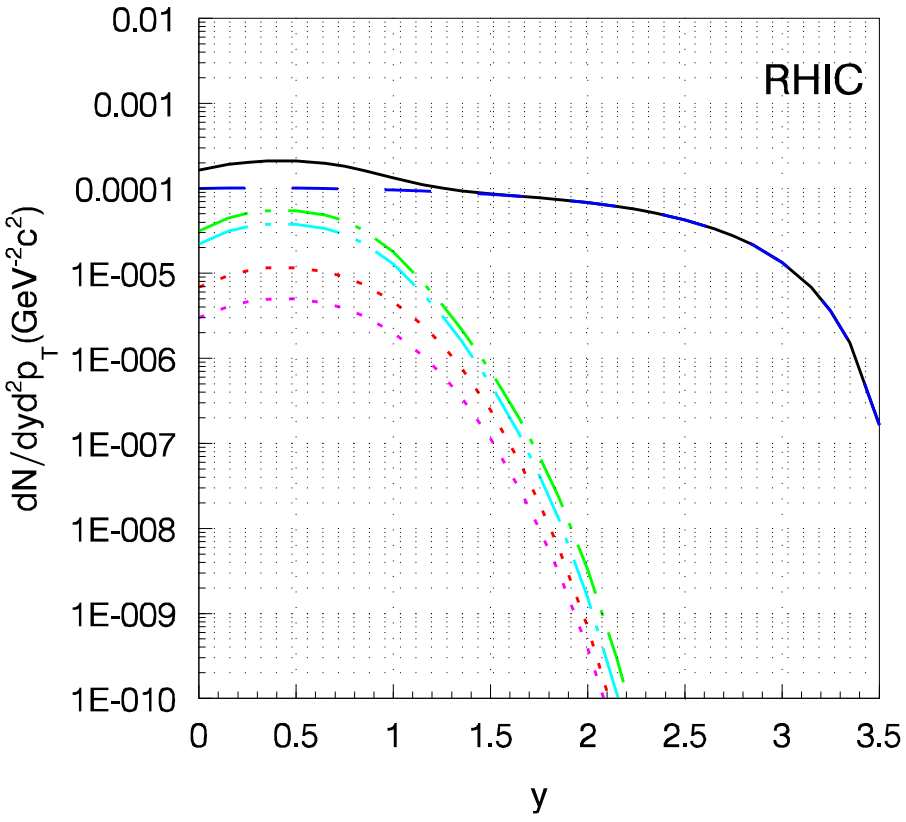

Figure 18: The same as Fig. 17, except for rapidity distribution at $p_T = 4$ GeV.

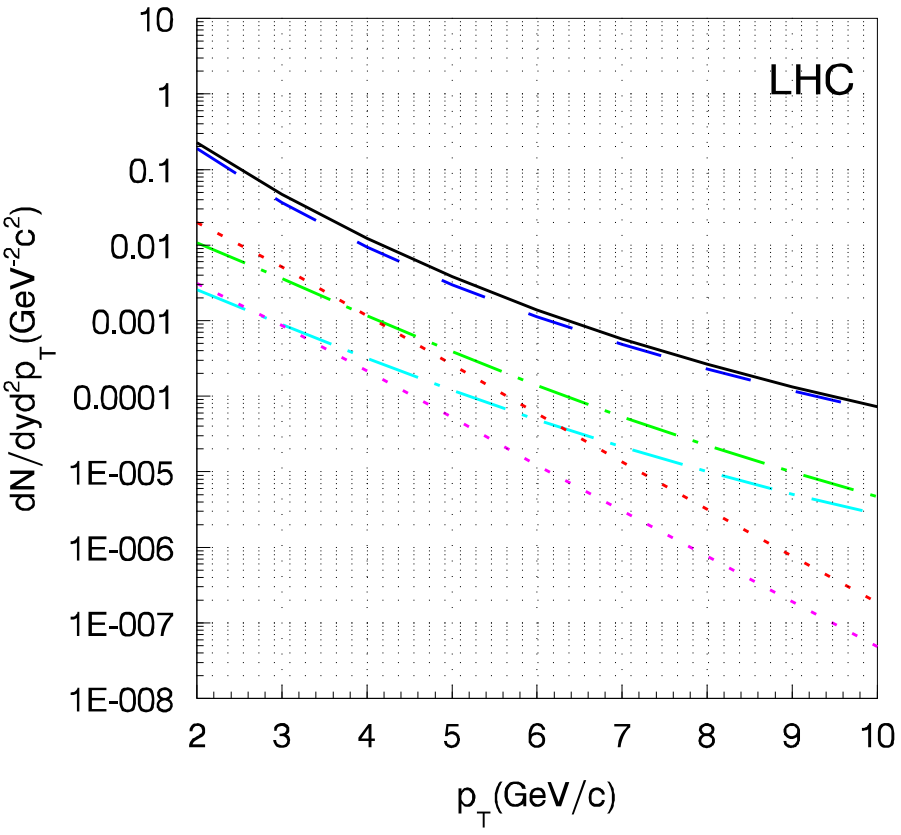

Figure 19: J/ψ number distributions versus transverse momentum at $y = 0$ and LHC energy without suppression. The dashed curve corresponds to $c\bar{c}$ productions in the initial collision. The upper and lower dot-dashed (dotted) curves correspond to $c\bar{c}$ produced through $2 \to 1$ and $2 \to 2$ reactions in the prethermal (thermal) stage, respectively. The solid curve is the sum of all contributions.

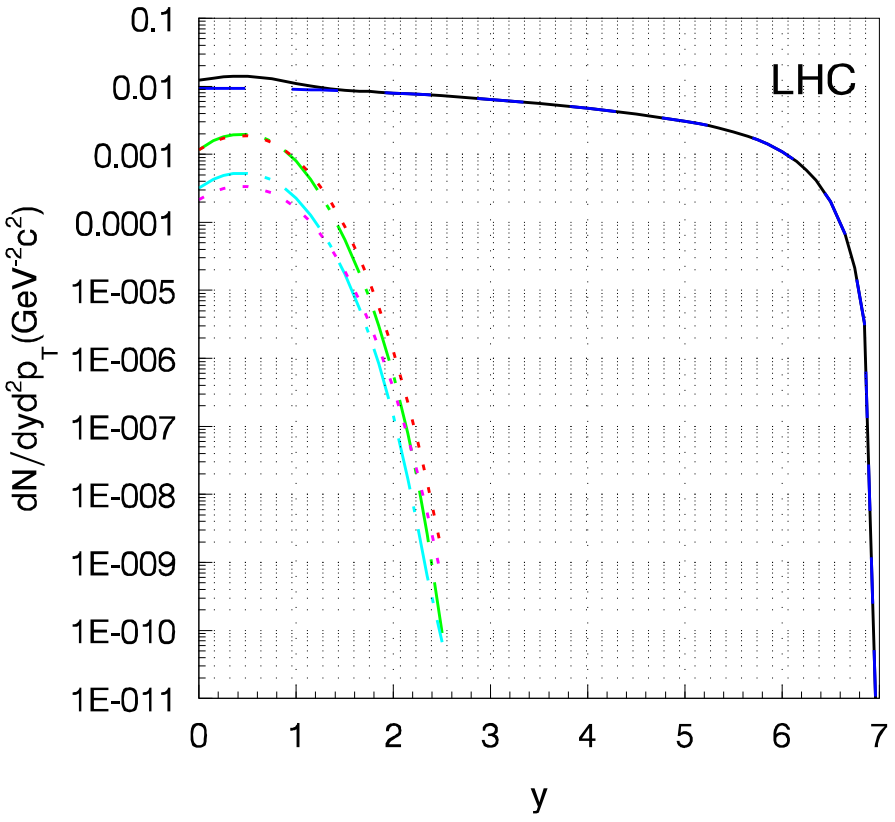

Figure 20: The same as Fig. 19, except for rapidity distribution at $p_T = 4$ GeV.

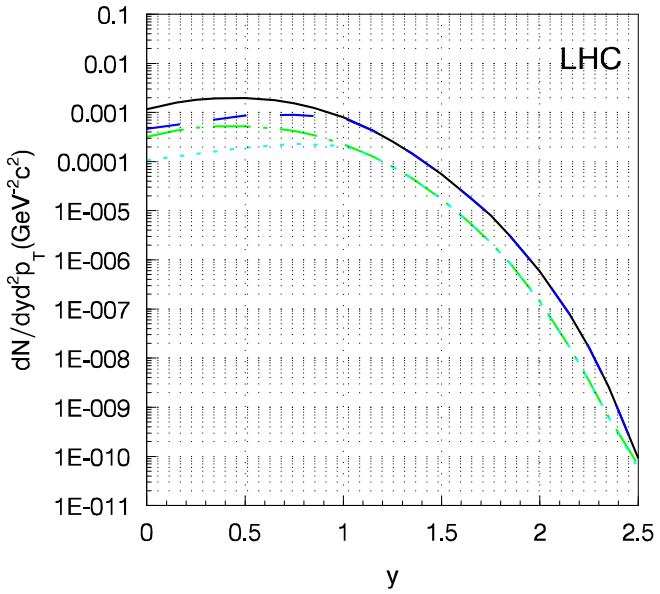

Figure 21: J/ψ number distributions versus rapidity at $p_T = 4$ GeV in the prethermal stage of LHC energy. The dashed and solid lines individually correspond to $c\bar{c}$ produced through $2 \to 1$ reactions with and without suppression. The dotted and dot-dashed lines through $2 \to 2$ reactions with and without suppression, respectively.

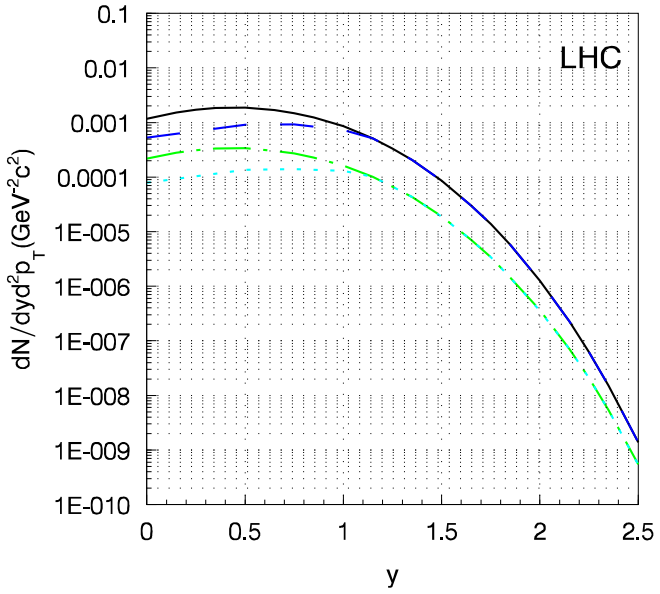

Figure 22: The same as Fig. 21, except for the thermal stage.

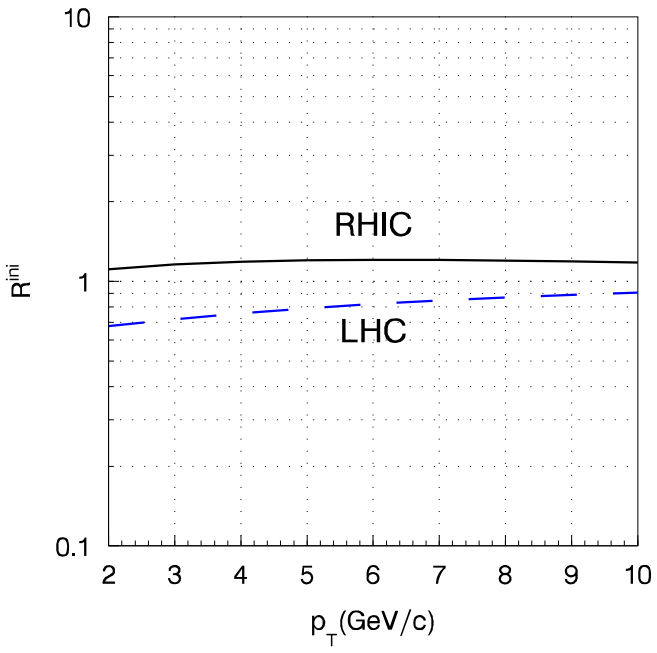

Figure 23: Ratio R^{ini} versus transverse momentum at $y = 0$ is calculated with Eskola's parametrization.

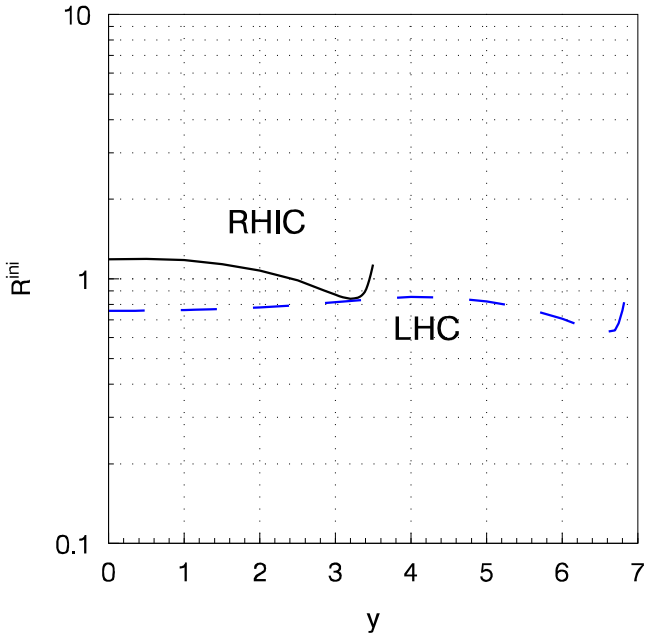

Figure 24: The same as Fig. 23, except for rapidity distribution at $p_T = 4$ GeV.